PHYSICAL REVIEW B VOLUME 44, NUMBER 4 15 JULY 1991-II

Strain energy and stability of Si-Ge compounds, alloys, and superlattices

James E. Bernard
2113 West Creighton Drive, Golden, Colorado 80401

Alex Zunger
Solar Energy Research Institute, Golden, Colorado 80401
(Received 28 December 1990)

First-principles total-energy pseudopotential calculations are carried out for Si, Ge, zinc-blende-structure SiGe, $(Si_2)_p/(Ge_2)_p$ superlattices in various layer orientations **G** and with various choices of substrate lattice parameter a_s, and for the $Si_{0.5}Ge_{0.5}$ random alloy. A subset of the results is used to construct an energy model, incorporating both strain (via an anharmonic valence force field) and chemical interactions (via a rapidly convergent cluster expansion) that closely reproduces the first-principles results, including those not used as input to the model. The model is applied to the study of larger superlattices than are amenable to first-principles treatment, revealing trends in (i) constituent strain energies, (ii) interfacial "strain-relief" relaxation energies, and (iii) interfacial chemical energies. The analysis reveals the major regularities in the dependence of superlattice stability on $\{p,\mathbf{G},a_s\}$, and permits investigation of the nature of interactions at interfaces, including the substrate-film interface.

I. INTRODUCTION

Ultrathin $(Si_2)_p/(Ge_2)_p$ superlattices (SL's) and Si_xGe_{1-x} films can be grown epitaxially in a variety of layer orientations, including (001),[1-4] (100),[5] and (111).[6] Provided that the films are thin enough, they can be made coherent with substrates of different lattice constants, ranging from that of Si (Refs. 1, 3, and 6) ($a=5.43$ Å), through Si_xGe_{1-x} alloys,[1,2,4] to that of Ge (Refs. 1, 5, and 7) ($a=5.66$ Å). Recent theoretical[8,9] and experimental[10] work has demonstrated how the choice of (i) superlattice-layer orientation **G**, (ii) superlattice repeat period $4p$, and (iii) substrate lattice parameter a_s sensitively affect the *electronic* properties: (i) and (ii) decide the number and symmetries of folded states, and (iii) controls strain-induced level shifts and splittings. Little is known,[8,9,11-15] however, about the way in which **G**, p, and a_s affect the *thermodynamic stability* of these binary SL's. While these parameters (along with growth conditions, surface steps, substrate misorientation, and surface reconstruction) can clearly affect growth *kinetics* and surface thermodynamics, we address here the complementary question of the relative *bulk thermodynamic* stabilities of already-grown binary SL's, e.g., short versus long, (001) versus (110) versus (111), and strained versus unstrained. Most previous systematic studies of thermodynamic stability of SL's (Refs. 16 and 17) treated *pseudobinary* $(AC)_p/(BC)_p$ systems with a common sublattice C. However, the *binary* $(A_2)_p/(B_2)_p$ system of diamondlike constituents studied here manifests new structural possibilities. For example, while there is a single type of (111) SL in the case of pseudobinary SL's, for binary SL's we distinguish two geometrical rhombohedral (RH) arrangements[18,19] [Figs. 1(a) and 1(b)]: the RH1 form, in which the interfaces occur within bilayers[20] along ⟨111⟩ containing one layer each of Si and Ge (intrabilayer or mixed-bilayer interfaces), and the RH2 form, in which the interfaces occur between bilayers (interbilayer or pure-bilayer interfaces).[21] For $p=1$ the bilayer sequence in RH1 is (SiGe)/(GeSi) $\cdots$, while in RH2 it is (SiSi)/(GeGe) $\cdots$.

In this paper we address the questions of the thermodynamic stability of coherent *binary* SL's versus $\{p,\mathbf{G}\}$, grown on different substrates. Total energies of SL's with given $\{p,\mathbf{G},a_s\}$ values can be obtained, for modestly small p values, from first-principles total-energy calculations,[22] e.g., within the local-density formalism.[23] The advantage of such approaches lies in the reliability with which these energies can be obtained. At the same time, the disadvantage is that the mere knowledge of the values of the total energies does not readily suggest the physical origins of stability or instability. Our main aim in this work is to use such first-principles calculations to construct simple models of SL stability that are both numerically reliable and physically transparent. In addition to general features of SL energetics, we calculate the formation enthalpy of the random alloy, compare it to that of various ordered structures, and consider the implications of our results regarding the interpretation of recent experiments in which spontaneous ordering of SiGe has been observed.[18,19]

The organization of the remainder of the paper is as follows. Section II introduces a simple physical model used to partition the SL formation enthalpy into strain and chemical components, which are analyzed in terms of bulklike and interfacelike contributions. Also introduced in Sec. II is the general approach to the calculation of the various contributions to the formation enthalpy and our model for calculating the formation enthalpy of a random SiGe alloy. Section III describes in detail the method used for calculating the strain energy of the SL's, including the first-principles calculations upon which it is based. Section IV presents the strain-energy results for

 ©1991 The American Physical Society

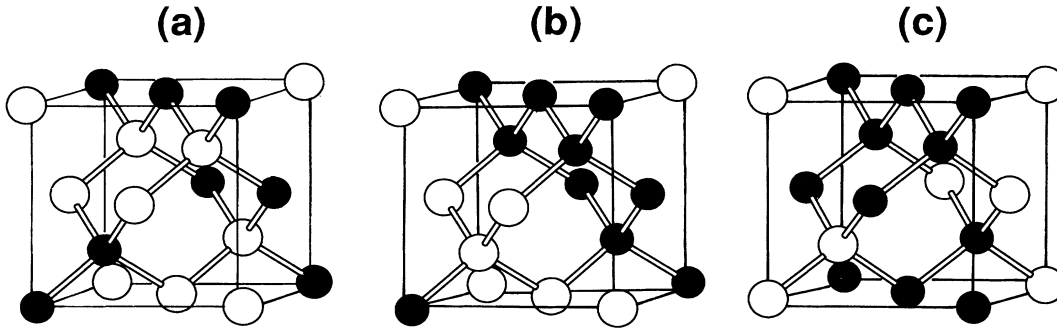

FIG. 1. The (a) RH1 $p=1$, (b) RH2 $p=1$, and (c) SQS-8 structures. Solid circles denote Si atoms, and open circles denote Ge atoms.

SL's and random 50%-50% alloys. Section V gives the model and results for chemical energies. Section VI adds up the strain and chemical contributions and discusses the emerging trends in the total formation energies as well as comparing the model results to analogous directly calculated first-principles results. Section VII discusses substrate-film interactions generally omitted from epitaxial calculations and considers under what circumstances they may be important. The energetics of some other interfaces are also considered. Section VIII considers the issue of abruptness of Si/Ge interfaces. Section IX summarizes our main results and discusses several issues regarding spontaneous ordering of SiGe alloys.

II. METHODOLOGY: A SIMPLE PHYSICAL MODEL AND ITS EVALUATION

A central quantity surrounding bulk thermodynamic stability is the formation enthalpy. We define the zero pressure formation enthalpy of a $(Si_2)_p/(Ge_2)_p$ SL, with repeat period $4p$, parallel (substrate) lattice constant a_s, and orientation $\mathbf{G}$, as its energy per atom taken with respect to the energies of equivalent amounts of its crystalline constituents Si and Ge at their bulk equilibrium lattice constants:

$$\Delta H(p,\mathbf{G},a_s)=E_{\rm SL}(p,\mathbf{G},a_s)-\tfrac{1}{2}[E_{\rm Si}(a_{\rm Si})+E_{\rm Ge}(a_{\rm Ge})]\ , \tag{1}$$

where $a_{\rm Si}$ and $a_{\rm Ge}$ are the equilibrium cubic lattice constants of Si and Ge, and the energies are all per atom. While our calculations of ΔH are based directly on this definition, the general form of $\Delta H(p,\mathbf{G},a_s)$ (neglecting small vibrational effects) and its scaling with p can be appreciated from simple considerations as follows. In pure Si and Ge, the nearest-neighbor bond lengths attain their "ideal" values $R_{\text{Si-Si}}=a_{\rm Si}\sqrt{3}/4$ and $R_{\text{Ge-Ge}}=a_{\rm Ge}\sqrt{3}/4$, and the bond angles have the "ideal" tetrahedral value $\Theta_{ijk}\approx 109.5°$. Imagine now forming the SL from its bulk constituents in two steps: first without allowing charge transfer, then with charge transfer.

The first contribution is termed "microscopic strain" and is constructed as follows. In the SL the bond lengths $\{r_{ij}\}$ and angles $\{\theta_{ijk}\}$ generally deviate from the ideal values $\{R_{ij}\}$ and $\{\Theta_{ijk}\}$, respectively, because topological constraints prevent simultaneous optimization of all structural degrees of freedom. The energy cost of the first step is the "microscopic strain" (MS) energy $\Delta E_{\rm MS}\ge 0$, resulting from this inability to accommodate in the SL the ideal bond geometry. SL's whose constituents are size matched (approximately true for, e.g., GaAs-AlAs) have[16] $\Delta E_{\rm MS}=0$. Since SL's with different layer orientations have different unit-cell structural parameters (e.g., types of interplanar spacings) compatible with their symmetries, they differ in the degree to which structural relaxations can relieve strain; hence $\Delta E_{\rm MS}=\Delta E_{\rm MS}(p,\mathbf{G},a_s)$. It is possible to partition $\Delta E_{\rm MS}$ into "bulk" and "interface" contributions[17] by considering the limit $p\to\infty$. A $(Si_2)_p/(Ge_2)_p$ SL has two interfaces per SL unit cell (containing $4p$ atoms); each interface contributes an interfacial "strain-relief" (SR) energy of $I_{\rm SR}(p,\mathbf{G},a_s)/2p$ per atom. In the $p\to\infty$ limit these interfaces contribute negligibly $[\sim O(1/p)]$ to ΔH, hence $\Delta E_{\rm MS}(p=\infty)$ is simply given by the elastic energy needed to deform the two constituents λ=Si,Ge from their cubic equilibrium structures [with lattice constants a_λ and energies $E_\lambda(a_\lambda)$] to the structure they attain inside the SL. This "constituent-strain" (CS) energy is

$$\Delta E_{\rm CS}(\mathbf{G},a_s)\equiv\Delta E_{\rm MS}(\infty,\mathbf{G},a_s)$$
$$=\sum_{\lambda\in\{\rm Si,Ge\}}[E_\lambda(\mathbf{G},a_s)-E_\lambda(a_\lambda)]\ , \tag{2}$$

where $E_\lambda(\mathbf{G},a_s)$ is the energy of component λ constrained to have the lattice constant a_s parallel to the substrate and relaxed in the perpendicular direction. Hence, for all p's the total microscopic strain energy (per atom) of a SL with structure $\alpha=\{p,\mathbf{G},a_s\}$ is

$$\Delta E_{\rm MS}^{(\alpha)}=\Delta E_{\rm CS}(\mathbf{G},a_s)+\frac{I_{\rm SR}(p,\mathbf{G},a_s)}{2p}\ . \tag{3}$$

Note that $\Delta E_{\rm CS}\ge 0$, since it represents deformation of the equilibrium structures of the *constituents,* whereas generally $I_{\rm SR}\le 0$, since it usually corresponds to relaxation of strained bonds in the *SL*. Note further that both $\Delta E_{\rm CS}$ and $I_{\rm SR}$ depend on the degree of size mismatch between the SL constituents. For *binary* $(A_2)_p/(B_2)_p$ SL's of size-mismatched constituents (e.g., Si and Ge) the two contributions of Eq. (3) cancel exactly only when there is

sufficient structural freedom to satisfy simultaneously the constraints $\{r_{ij}\}=\{R_{ij}\}$ and $\{\theta_{ijk}\}=\{\Theta_{ijk}\}$. Such "topologically unconstrained"[12] systems include the RH1 SL with $p=1$ [Fig. 1(a)] and the zinc-blende (ZB) structure. In contrast, all lattice-mismatched *pseudobinary* $(AC)_p/(BC)_p$ adamantine SL's with a common sublattice C are "topologically constrained,"[24] and so have $\Delta E_{\mathrm{MS}}>0$.

In the *second* step of forming a SL, one allows for charge exchange (CE), associated with an energy $I_{\mathrm{CE}}(p,\mathbf{G})$ per interface, or $I_{\mathrm{CE}}(p,\mathbf{G})/2p$ per atom. This primarily reflects the formation of Si—Ge bonds but also the creation of altered chemical environments around Si—Si and Ge—Ge bonds. This "chemical energy" of isovalent SL's is hence

$$\Delta E_{\mathrm{chem}}(p,\mathbf{G})]=\frac{I_{\mathrm{CE}}(p,\mathbf{G})}{2p} . \quad (4)$$

The total formation enthalpy of Eq. (1) can be thought of as a sum of strain-energy and chemical-energy terms:

$$\Delta H(p,\mathbf{G},a_s)=\Delta E_{\mathrm{MS}}(p,\mathbf{G},a_s)+\Delta E_{\mathrm{chem}}(p,\mathbf{G}) , \quad (5)$$

or, alternatively, as a sum of bulklike and interfacelike terms:

$$\Delta H(p,\mathbf{G},a_s)=\Delta E_{\mathrm{CS}}(\mathbf{G},a_s)+\frac{1}{2p}[I_{\mathrm{SR}}(p,\mathbf{G},a_s)+I_{\mathrm{CE}}(p,\mathbf{G})] . \quad (6)$$

While, in general, formation enthalpies could be partitioned in a number of different ways,[25] we will see below that the definitions underlying Eqs. (2)–(6) are particularly useful for describing the physical ingredients of SL stability. In particular, this analysis shows that (i) the relative stability of *long-period* SL's is governed by the constituent strain energy [first term in Eq. (6)] and could differ from that of *short-period* SL's where the interfacelike terms [bracketed in Eq. (6)] may be important. (ii) The asymptotic limit of $\Delta H(p\rightarrow\infty)=\Delta E_{\mathrm{CS}}(\mathbf{G},a_s)$ vanishes for size-matched SL's and is positive for size-mismatched SL's. The limit could be approached either from below or from above, depending on whether the interfaces are attractive ($I_{\mathrm{SR}}+I_{\mathrm{CE}}<0$) or repulsive ($I_{\mathrm{SR}}+I_{\mathrm{CE}}>0$).

The *total* formation enthalpy can be calculated quantum mechanically directly from Eq. (1) using self-consistent electronic-structure techniques,[22,23] which treat chemical and elastic interactions on an equal footing. This is currently feasible[16,17] computationally only for SL's with a modest number of atoms per cell ($4p\leq 20$) and for $p=\infty$ [deformed constituents, Eq. (2)]. Our primary aim here, however, is to analyze the factors governing stability, by considering a range of p's, $\mathbf{G}$'s, and a_s's. We do this as follows.

(i) The microscopic strain energy ΔE_{MS} is calculated classically for a large range of p's by optimizing the elastic energy of a SL as a function of its structure, given a force field. We use a generalized form of Keating's valence force field[26,27] (VFF), which expresses ΔE_{MS} for an arbitrary adamantine structure in terms of the ideal $\{R_{ij}\}$, $\{\Theta_{ijk}\}$, and a set of bond-stretching and bond-bending force constants. Our generalized VFF model, the details of which are presented in Sec. III B, includes anharmonic terms of both the bond-stretching and bond-bending types. The parameters of this anharmonic VFF (AVFF) model were obtained by fitting the results of first-principles self-consistent pseudopotential total-energy calculations (described in Sec. III A) for bulk and epitaxially deformed Si, Ge, and zinc-blende-structure SiGe to the model. The details of the fitting procedure and specific values resulting from the fits are discussed in Sec. III B. We calculate $\Delta E_{\mathrm{MS}}^{(\alpha)}$ from this "first-principles AVFF" for various $\alpha=\{p,\mathbf{G},a_s\}$ by directly relaxing the coordinates of the $4p$ atoms per cell and any appropriate cell-external degrees of freedom using a conjugate-gradient optimization method.[28] The results are described in Sec. IV. (ii) The same calculation for the deformed pure constituents gives ΔE_{CS}; the difference $\Delta E_{\mathrm{MS}}-\Delta E_{\mathrm{CS}}$ then provides $I_{\mathrm{SR}}/2p$. (iii) First-principles total-energy calculations for the topologically unconstrained ($\Delta E_{\mathrm{MS}}\equiv 0$) zinc-blende and RH1 ($p=1$) structures give directly $\Delta E_{\mathrm{chem}}^{(\alpha)}=\Delta H^{(\alpha)}$. These are then used to define a cluster expansion of ΔE_{chem} in terms of first- and second-neighbor pair interactions. We will see below that the charge-transfer effects underlying ΔE_{chem} give rise to relatively short-range interactions, so that these two terms are sufficient to give reasonably good convergence. Having determined the cluster interactions from the pseudopotential total energies, we can predict the chemical energies of *arbitrary* structures. The details of the cluster expansion and the determination of the coefficients are presented in Sec. V.

To test the overall numerical accuracy of the model we combine $\Delta E_{\mathrm{MS}}^{(\alpha)}$ obtained from the AVFF model with $\Delta E_{\mathrm{chem}}^{(\alpha)}$ obtained from the cluster expansion and compare (for structures *not used* to deduce the interaction parameters of the cluster expansion) the result to directly calculated first-principles formation enthalpies. We will see below that the agreement is excellent, thus substantiating the accuracy of the model. This analysis then permits calculation of the three physical terms—ΔE_{CS}, I_{SR}, and I_{CE} (or ΔE_{chem})—governing the stability of these SL's. Furthermore, this analysis allows us to predict ΔH for structures that are too complicated to calculate directly from first principles.

In addition to the formation enthalpies of the ordered SL's, an analysis of thermodynamic stability requires the mixing enthalpy of the random $\mathrm{Si}_x\mathrm{Ge}_{1-x}$ alloy. We calculate the enthalpy of formation of a random alloy via the "special-quasirandom-structure" (SQS) concept.[29] The basic idea is that within a relatively small supercell with N atomic sites, we select the set of occupations by Si and Ge that most closely mimics the short-range radial correlation functions of a perfectly random infinite alloy. This is done by determining the multisite correlation functions of each possible structure within a given N, and choosing the structure with the best match to those of a random alloy. For the $\mathrm{Si}_{0.5}\mathrm{Ge}_{0.5}$ alloy, we use an eight-atom SQS, shown in Fig. 1(c). This is a (2,2) SL along the [110] direction on each of the two fcc sublattices of the

diamond structure, with a particular choice of "phase" between the two SL's. As a check of the quality of this SQS, we also calculate the strain energy of a number of large random supercells, where 1000 Si and Ge atoms are distributed randomly on a diamondlike lattice, and the relaxed energies are averaged over many distinct configurations of the random system. We find that a calculation on SQS-8, with just eight atoms per cell, closely reproduces the results of this direct simulation with 1000 atoms per cell, thus substantiating the SQS construct. These results are discussed in Sec. IV.

The complete analysis of SL formation enthalpies and random alloy mixing enthalpies in terms of our model of Eqs. (5) and (6) then permits assessment of thermodynamic stability of various phases. This is discussed in Sec. VI.

III. METHOD OF CALCULATION

A. First-principles pseudopotential calculations

Our first-principles self-consistent plane-wave pseudopotential calculations[22] were done in the local-density approximation[23] with a plane-wave energy cutoff of 20 Ry, using in all cases the equivalent of 10 special **k** points[30] in the irreducible part of the diamond Brillouin zone. The use of equivalent basis sets, **k**-point sampling, and self-consistency for all structures results in a *relative* precision of ΔH's for near-equilibrium structures of about 0.1 MeV/atom (whereas absolute accuracy is not as good).

For determination of the AVFF parameters, we did four sets of seven total-energy calculations for each of the three materials, Si, Ge, and zinc-blende-structure SiGe: one set scanning the volume (maintaining a cubic cell), and three sets being done under coherent epitaxial conditions, where the substrate lattice constant in the (001) plane was held at approximately the equilibrium lattice constant of Si, Ge, or their average, and the c/a ratio was varied. The range of the cubic scans was about $\pm 15\%$ of the equilibrium volume, and that of the epitaxial scans was $\pm 9\%$ in the c/a ratio.

In a number of the first-principles calculations the structural distortions caused the materials to become metallic. In addition, it is not possible to preserve absolute equivalence in **k**-point sampling under the distortions involved in the scans (we distort the sampling mesh along with the unit cell, to preserve both the number of mesh points and the topology of the mesh in the full Brillouin zone). As a result of these and other sources of noise in the first-principles scans, all fits of these results were done with weights applied to the scan points, giving gradually decreasing weight to points further from the energy minimum, and reducing the weight for metallic cases by an additional factor of 2. All fits were done using χ^2 minimization.

Table I summarizes the results of the scans. The equilibrium lattice constants were determined by fitting the results of the volume (cubic) scans to a Birch equation of state.[31] The bulk moduli and epitaxial strain-reduction factors

$$q(\mathbf{G})=\frac{E(\mathbf{G},a_s,c_{\mathrm{eq}})-E(a_{\mathrm{eq}})}{E(\mathbf{G},a_s,c=a_s)-E(a_{\mathrm{eq}})} \tag{7}$$

(where the subscript "eq" denotes equilibrium values, and the c-axis dependence is made explicit for the epitaxial energies) were determined from the second-order elastic constants C_{11} and C_{12} resulting from fitting to a third-order elastic model. The equilibrium c-axis lengths were determined from fits of the individual epitaxial (c/a) scans to a third-order elastic model including only terms in C_{11} and C_{111}. We find that equilibrium c-axis lengths determined from harmonic elasticity theory[32]

$$c_{\mathrm{eq}}([001],a_s)=a_{\mathrm{eq}}-\{2-3q([001])\}(a_s-a_{\mathrm{eq}}) \tag{8}$$

agree to better than 0.1% with those given in Table I, though the effects of anharmonicity would cause energies calculated from harmonic elasticity theory to be considerably less reliable. Note also that for any two substrate lattice constants, $[c_{\mathrm{eq}}(a_2)-c_{\mathrm{eq}}(a_1)]/(a_2-a_1)<0$, showing the expected behavior that the c axis relaxes to compensate changes in a_s, thus tending to preserve the volume of the equilibrium cubic structure.

Our determination of ΔE_{chem} in Sec. V utilizes the results of first-principles calculations for the bulk ZB and RH1 $p=1$ structures. Here we discuss those first-principles results as well as the analogous epitaxial results and those for the related RH2 $p=1$ structure, and compare them to previous calculations. Our pseudopotential calculations for the equilibrium "bulk" ZB and RH1 $p=1$ structures give $\Delta H=9.9$ and 6.5 meV/atom. Martins and Zunger,[12] in a pseudopotential calculation with a plane-wave energy cutoff of 18 Ry, and the equivalent of two special **k** points in the irreducible wedge of the diamond Brillouin zone found 7.6 meV/atom and 6.6 meV/atom, respectively. In a separate 24 Ry, 10-**k**-point calculation, they found for the ZB structure $\Delta H=8.9$ meV/atom. Dandrea,[33] who used the same energy cutoff and **k**-point sampling used here, found 6.8 meV/atom for

TABLE I. Pseudopotential-calculated bulk moduli B (GPa), epitaxial strain-reduction factors q [Eq. (7)] for [001]-oriented substrates, equilibrium lattice constants a_{eq} (Å), and equilibrium unit-cell c-axis length (Å) for three [001]-oriented substrates with a_s approximately equal to the lattice constants of Si, Ge, and their average. ZB denotes zinc-blende-structure SiGe.

	B	q([001])	a_{eq}	c_{eq} $a_s=5.3956$	c_{eq} $a_s=5.4908$	c_{eq} $a_s=5.5861$
Si	96.0	0.40	5.3946	5.3937	5.3185	5.2429
ZB SiGe	86.6	0.41	5.4799	5.5426	5.4714	5.4004
Ge	76.0	0.42	5.5835	5.7169	5.6487	5.5799

RH1 $p=1$. For RH2 $p=1$, we find 9.2 meV/atom, while Dandrea found 9.5. On a (001) Si substrate, we find 14.9, 11.7, and 11.7 meV/atom for ZB, RH1 $p=1$, and phase-separated Si+Ge, respectively. The corresponding values found in Ref. 12 are 13.3, 10.9, and 13.0 meV/atom, respectively. While these differences are small, there is a qualitative difference in that we find strained RH1 $p=1$ to be degenerate with its strained constituents within the precision of our calculation, whereas Ref. 12 finds strained RH1 $p=1$ to be more stable by about 2 meV/atom.

B. The anharmonic VFF model

The microscopic strain energy of Eq. (5) is evaluated from a purely elastic model that represents the increase in energy due to stretching and bending of ideal bond lengths and angles. The AVFF energy expression follows the general form outlined by Keating,[26] in being an expansion in terms of quantities

$$\lambda_{ijkl}=(\mathbf{r}_{ij}\cdot\mathbf{r}_{kl}-\mathbf{R}_{ij}\cdot\mathbf{R}_{kl})/d$$

depending on interatomic displacement vectors $\mathbf{r}_{ij}$, their ideal values $\mathbf{R}_{ij}$, and a length scale d of the order of an ideal bond length, the subscripts being atom indexes. Following Keating we keep only nearest-neighbor-pair bond-stretching interactions (involving $\lambda_{ij}\equiv\lambda_{ijij}$) and nearest-neighbor-triplet bond-bending interactions (involving $\lambda_{ijk}\equiv\lambda_{ijik}$), but we incorporate anharmonicity by allowing terms higher than λ^2 to be kept in the expansion. The resulting expression for the elastic energy per unit cell is

$$E=\frac{1}{2}\sum_{i=1}^{N_a}\sum_{j=1}^{N_i}\left[\sum_{n=2}^{M_s}\frac{1}{n!}\left[\frac{\sqrt{3}}{2}\right]^n\alpha_{ij}^{(n)}\lambda_{ij}^n\right]+\sum_{i=1}^{N_a}\sum_{j=1}^{N_i}\sum_{k=j+1}^{N_i}\left[\sum_{n=2}^{M_b}\frac{1}{n!}\left[\frac{\sqrt{3}}{2}\right]^n\beta_{ijk}^{(n)}\lambda_{ijk}^n\right], \quad (9)$$

where N_a is the number of atoms per unit cell, N_i is the number of nearest neighbors to atom i (always four in adamantine structures), M_s is the highest-order bond-stretching term kept, M_b is the highest-order bond-bending term kept, $\alpha_{ij}^{(n)}$ is an nth-order bond-stretching force constant, $\beta_{ijk}^{(n)}$ is an nth-order bond-bending force constant, and the outer factor of $\frac{1}{2}$ in the bond-stretching term compensates for double counting of the bonds. The bond-stretching λ's are

$$\lambda_{ij}=\frac{(r_{ij}^2-R_{ij}^2)}{R_{ij}}, \quad (10)$$

and the bond bending λ's are

$$\lambda_{ijk}=\frac{(\mathbf{r}_{ij}\cdot\mathbf{r}_{ik}-\mathbf{R}_{ij}\cdot\mathbf{R}_{ik})}{(R_{ij}R_{ik})^{1/2}}, \quad (11)$$

where the scale d has been chosen to be the geometric means of the ideal bond lengths of the two bonds. In the usual (harmonic) VFF method, $M_s=M_b=2$.

The AVFF force constants were determined by fitting the pseudopotential results of all four scans for each compound to the AVFF model, fixing the $\{R_{ij}\}$ at the values determined by the Birch[31] fits for the cubic systems and the $\{\Theta_{ijk}\}$ at the ideal tetrahedral angle. We found that keeping terms beyond $M_s=M_b=4$ provided little additional improvement in the fit to the first-principles energies near the minima of the scans. However, the use of AVFF parameters derived from fits with $M_s=M_b=4$ in structural optimizations resulted in disintegration of the structures, because the energy could become negative for large atomic separations. By restricting $M_b=3$ (except for Si, for which $M_b=4$ could be used), we were able to obtain stable structures with little deterioration of the quality of the fits near the minima of the first-principles scans. With AVFF parameters derived in this way (Table II), the first-principles strain energies near the minima of the scans were reproduced to within 0.25 meV/atom. To demonstrate the quality of the fit, consider the four geometries of epitaxial Ge: (1) $a_s=\bar{a}$, $c/a=1.03$, (2) $a_s=a_{\mathrm{Ge}}$, $c/a=0.97$, (3) $a_s=a_{\mathrm{Si}}$, $c/a=1.03$, and (4) $a_s=\bar{a}$, $c/a=0.97$. Here a_{Si}, $\bar{a}$, and a_{Ge} refer to the three substrate lattice constants given in the heading of Table I. (In all of these cases, pseudopotential calculations show that Ge is nonmetallic, so our **k**-point sampling is adequate.) We calculated for each of these external constraints the pseudopotential and AVFF total energies (given in parentheses). For (001) Ge, we find in meV: 5.3(5.4), 7.4(7.3), 31.8(31.9), and 38.2(38.1) for cases 1–4, respectively. Since no (110) data was used in the fit, it is interesting to examine the extent to which this AVFF predicts (110) deformed energies. We use the VFF parameters of Table III to relax the cell-internal geometrical parameters. We find for (110) Ge: 6.8(6.2), 9.4(9.3), 33.3(32.9), and 40.2(40.1) for cases 1–4, respectively. While the fit is slightly worse than for (001), it is still clearly quite good.

For comparison, Table III gives second-order elastic constants and harmonic VFF parameters derived from

TABLE II. Parameters for the anharmonic VFF model [Eq. (9)], derived from fits (described in Sec. III A) of pseudopotential total-energy calculations for Si, Ge, and zinc-blende-structure SiGe. Equilibrium bond lengths R_{ij} are in Å, and force constants $\alpha_{ij}^{(n)}$ and $\beta_{ijk}^{(n)}$ are in N/m^{n-1}.

Bond-stretching parameters					
Atoms i	j	R_{ij}	$\alpha_{ij}^{(2)}$	$\alpha_{ij}^{(3)}$	$\alpha_{ij}^{(4)}$
Si	Si	2.3359	46.28	−154.88	540.13
Ge	Ge	2.4177	38.57	−128.58	260.25
Ge	Si	2.3729	42.71	−150.38	381.62

Bond-bending parameters					
i	Atoms j	k	$\beta_{ijk}^{(2)}$	$\beta_{ijk}^{(3)}$	$\beta_{ijk}^{(4)}$
Si	Si	Si	12.83	46.28	373.89
Ge	Ge	Ge	10.59	57.35	
Ge	Si	Ge	12.14	20.80	
Si	Ge	Si	12.14	20.80	
Si	Si	Ge	12.49	33.54	186.94
Si	Ge	Ge	11.37	39.07	

TABLE III. First-principles-derived second-order elastic constants C_{11} and C_{12} and harmonic VFF parameters, and experiment-derived harmonic VFF parameters. Elastic constants are in GPa, equilibrium bond lengths R_{ij} are in Å, and force constants are in N/m.

Elastic constants and bond-stretching parameters					
Atoms					
i	j	C_{11}	C_{12}	R_{ij}	$\alpha_{ij}^{(2)}$
			First principles		
Si	Si	159.5	64.2	2.3359	47.49
Ge	Ge	131.2	48.4	2.4177	38.58
Ge	Si	147.8	56.1	2.3729	43.29
			Experiment[a]		
Si	Si	165.7	63.9	2.352	48.50
Ge	Ge	128.9	48.3	2.450	38.67

Bond-bending parameters			
	Atoms		
i	j	k	$\beta_{ijk}^{(2)}$
			First principles
Si	Si	Si	12.86
Ge	Ge	Ge	11.55
Ge	Si	Ge	12.57
Si	Ge	Si	12.57
Si	Si	Ge	12.72
Si	Ge	Ge	12.06
			Experiment[a]
Si	Si	Si	13.82
Ge	Ge	Ge	11.37

[a]From compilation in Ref. 27.

our first-principles results and from experimental data compiled in Ref. 27. The derivation from the first-principles results was done by fitting to a third-order elastic model using χ^2 minimization with the same weights used for the AVFF fits. The resulting second-order elastic constants (Table III) were then used to determine the VFF force constants, in the manner described by Keating.[26] This procedure is very similar to that followed by Froyen, Wood, and Zunger.[9] We note that generally the corresponding AVFF force constants are slightly smaller than either the first-principles or experimental VFF force constants. These harmonic VFF force constants are not used in any of the calculations described in this paper, and are presented only for reference. We note that the ideal bond lengths determined by Froyen, Wood, and Zunger[9] in their series of pseudopotential calculations using a plane-wave energy cutoff of 12 Ry and six special **k** points in the irreducible part of the diamond Brillouin zone are less than 0.5% larger than ours, their VFF bond-stretching force constants are about 1% smaller than ours, and their VFF bond-bending force constants are 5–11% larger than ours.

IV. RESULTS FOR MICROSCOPIC STRAIN ENERGIES

A. Superlattices on lattice-matched substrates

Figure 2(a) depicts $\Delta E_{\rm MS}(p,\mathbf{G},\bar{a})$ for $\mathbf{G}=[001]$, [110], and [111] on a lattice-matched substrate whose lattice constant a_s is taken to be the average of the Si and Ge lattice parameters (essentially the natural equilibrium SL lattice parameter $a_{\rm SL}$), describing free-standing bulk SL's. The third and fifth columns of Table IV summarize the results for $I_{\rm SR}(\infty)$, $\Delta E_{\rm CS}(\mathbf{G},\bar{a})$, and $\Delta E_{\rm MS}(p,\mathbf{G},\bar{a})$.

Considering first the long period ($p\rightarrow\infty$) limit, we find [Fig. 2(a)] the stability sequence

$$\Delta H(\infty,[001])<\Delta H(\infty,[110])<\Delta H(\infty,[111])\ , \qquad (12)$$

as in lattice-mismatched pseudobinary III-V and II-VI SL's.[17] This can be understood from harmonic elasticity theory,[17,23] where the energy density U of a coherently strained film is written as a quadratic form in the strains $\epsilon_\parallel$ and $\epsilon_\perp$ parallel and perpendicular to the substrate. The condition $dU/d\epsilon_\perp=0$ for fixed $\epsilon_\parallel$ gives the constituent strain energy of Eq. (2) per atom

$$\Delta E_{\rm CS}(a_s,\mathbf{G})=\sum_\lambda \tfrac{9}{16}q_\lambda(\mathbf{G})B_\lambda a_\lambda(a_s-a_\lambda)^2\ , \qquad (13)$$

where $B=(C_{11}+2C_{12})/3$ is the bulk modulus, C_{ij} are elastic constants, and all orientation dependence lies in the epitaxial strain-reduction factor

$$q(\mathbf{G})=1-B/[C_{11}+\gamma(\mathbf{G})\Delta]\ . \qquad (14)$$

Here, $\Delta=C_{44}-(C_{11}-C_{12})/2$ is the elastic anisotropy, and $\gamma([001])=0$, $\gamma([110])=1$, and $\gamma([111])=\frac{4}{3}$. Note that the coefficient $9B_\lambda a_\lambda/16$ appearing in *hydrostatic* equations of state[32] is replaced in the epitaxial case of Eq. (13) by $9q_\lambda B_\lambda a_\lambda/16$. The "effective" epitaxial modulus $q_\lambda B_\lambda$ shows softening ($q<1$), as illustrated in Table I.

TABLE IV. Constituent strain energy $\Delta E_{\rm CS}$ (meV/atom) and $p\rightarrow\infty$ chemical ($I_{\rm CE}$), strain-relief ($I_{\rm SR}$), and total (I) interfacial energies (meV/primitive-cell interface) of Eq. (6) for superlattices on lattice-matched ($a_s=\bar{a}$) and lattice-mismatched ($a_s=a_{\rm Si}$) substrates with orientation parallel to the superlattice stacking direction.

			$a_s=\bar{a}$			$a_s=a_{\rm Si}$	
System	$I_{\rm CE}(\infty)$	$I_{\rm SR}(\infty)$	$I(\infty)$	$\Delta E_{\rm CS}$	$I_{\rm SR}(\infty)$	$I(\infty)$	$\Delta E_{\rm CS}$
(001)	7.52	−6.10	1.42	5.89	−6.92	0.60	11.70
(110)	6.31	−9.47	−3.16	7.05	−5.21	1.10	12.07
RH1	13.08	−14.77	−1.69	7.47	−16.25	−3.17	14.43
RH2	3.16	0.09	3.24	7.47	0.27	3.42	14.43

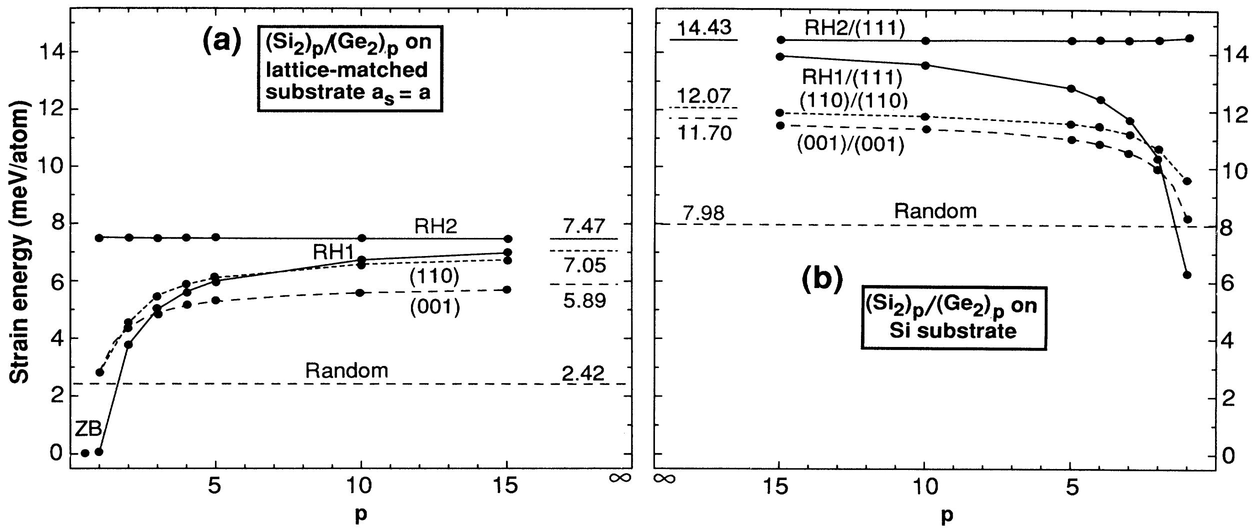

FIG. 2. Strain energy of SiGe superlattices and the random alloy on (a) lattice-matched substrates $a_s = \bar{a} = 5.4890$ Å and (b) Si substrates $a_s = a_{Si} = 5.3946$ Å.

Since $\Delta > 0$ for Si and Ge, the order of Eq. (12) simply reflects the order of the geometric factors $\gamma(\mathbf{G})$. Table IV gives the ΔE_{CS} values.

For short-period SL's the microscopic strain energy reflects [Eq. (3)] both interfacial relaxations (SR) and constituent strain (CS). Considering our results at $a_s = \bar{a} \cong a_{SL}$, we see that (i) RH1 has $\Delta E_{MS} \cong 0$ for $p = 1$ [Fig. 2(a)], i.e., it is indeed[12] a topologically unconstrained structure where the SR exactly compensates the CS (the energy vanishes at $a_s = a_{SL}$). This can be understood geometrically by realizing that the mixed bilayers that constitute the interfaces in RH1 [Fig. 1(a)] have the Si—Ge bond lengths and angles fully relaxed at the SL lattice constant (essentially the same as that of zinc-blende-structure SiGe), and the bilayers are then free to adjust along [111] until both the Si—Si and Ge—Ge bonds joining them are fully relaxed, with *no cost* in bond-angle strain, since these bonds are aligned along [111]. For $p > 1$ some of the bilayers contain only a single type of atom, so they must be strained (at the SL lattice constant); thus the energy increases with p as the proportion of pure bilayers increases. (ii) RH1 has lower strain energy than (001) up through $p = 2$; it has lower strain energy than (110) up through about $p = 7$. (iii) (001) and (110) SL's on lattice-matched substrates are geometrically identical at $p = 1$; thereafter, the (001) SL consistently has lower strain energy for all p's. (iv) RH2 has the highest strain energy for all p's. This can be understood geometrically by contrasting it with RH1. In RH2 all the bilayers contain only a single type of atom [Fig. 1(b)], and these bilayers are thus highly strained at the SL lattice constant. Interbilayer relaxation successfully removes essentially all strain from the Si—Ge bonds (oriented along [111]), but this cannot affect the intrabilayer strain, whose relaxation is determined by the balance between bond-stretching and bond-bending forces *within the bilayers* themselves. Hence the strain energy is nearly independent of p, the proportion of pure bilayers being 100% for all p.

Since RH1 and RH2 have the same epitaxial strain-reduction factor $q(\mathbf{G})$ [Eq. (14)], they also have the same constituent strain energy ΔE_{CS} (Table IV); hence the difference in their strain energies, $I_{SR}/2p$ for finite p [Fig. 2(a)], must be reflected in more favorable interfacial strain-relief energies (I_{SR}) in the former. Our fit of the AVFF results of Fig. 2(a) at $a_s = \bar{a}$ to Eq. (3) (for large p) shows (Table IV) that indeed the RH2 interface does not relieve the constituent strain ($I_{SR} \cong 0$), while the others do so at least partially ($I_{SR} < 0$).

B. Superlattices on lattice-mismatched substrates

Figure 2(b) depicts the microscopic strain energies for SL's on a Si substrate with orientation $\mathbf{G}_s$ parallel to the SL stacking direction $\mathbf{G}$; the Ge portion of the SL is now strained, with energy proportional to $(\Delta a)^2 = (a_{Ge} - a_{Si})^2$, whereas the Si part is unstrained (except near the interface). This raises the constituent strain energy [Fig. 2(b) and Table IV] relative to the case $a_s = \bar{a}$ [Fig. 2(a)], where both Si and Ge were strained, each with energy proportional to $(\Delta a)^2/4$. The constituent strain energy for (001), 11.7 meV/atom, agrees well with our pseudopotential calculations for the same orientation, which also give 11.7 meV/atom, and is in reasonable agreement with the value of 13.0 meV/atom found by Martins and Zunger[12] (it is in worse agreement with the value of 9.9 meV/atom found by Ciraci and Batra[13] who used a smaller basis set than was used here or in Ref. 12). On the Si substrate [Fig. 2(b)], we find that RH1 has lower strain energy than the (110) SL's only up through $p = 2$ (compared to about $p = 7$ for $a_s = \bar{a}$); it has lower strain energy than the (001) SL's only for $p = 1$. The latter SL's have lower strain energy than (110) for *all* p's (including $p = 1$).

The interfacial strain-relief energies of these epitaxial

SL's on Si substrates (Table IV) show similar trends to those of the SL's on $a_s = \bar{a}$, RH1 having the largest (magnitude) $I_{SR}(\infty)$, RH2 the smallest, and the others intermediate. Generally the magnitudes of $I_{SR}(\infty)$ are slightly larger here than those extracted from the calculations for the SL's on a lattice-matched substrate, an exception being the (110) SL's.

C. Summary of strain energies of $p = 1$ superlattices on different substrates

Our AVFF results for $p = 1$ are summarized in Fig. 3. It shows that while all SL's have greater elastic energies than equivalent amounts of *bulk* Si+Ge (the zero of energy), when strained epitaxially on Si their strain energy is (except for RH2) lower than that of the coherent constituents (far right column in Fig. 3). This effect has been termed[12,32] "epitaxial stabilization." The relevant *epitaxial* formation enthalpy here is taken with respect to pure *A* and pure *B both coherent with the substrate:*

$$\delta H(p, \mathbf{G}, a_s) = E_{SL}(p, \mathbf{G}, a_s) - \tfrac{1}{2}[E_{Si}(a_s) + E_{Ge}(a_s)] , \quad (15)$$

where all energies are per atom. We see from Eqs. (1), (2), (6), and (15) that $\delta H = (I_{SR} + I_{CE})/2p$. Indeed, RH1 has the largest epitaxial stabilization on a Si substrate, resulting in epitaxial formation enthalpies (including strain only) of $\delta H((111)) = -8.1$ meV/atom on (111) Si and $\delta H((001)) = -6.5$ meV/atom on (001) Si. For the (001) SL $\delta H((001)) = -3.5$ meV/atom, and for the (110) SL $\delta H((110)) = -2.5$ meV/atom. This is qualitatively different from the behavior in lattice-mismatched pseudobinary III-V and II-VI SL's,[17] where $\delta H < 0$ for (mixed-cation) (001) and (110) SL's but not for (111). Here the RH2 SL's behave like the pseudobinary (111) SL's

We have also calculated the strain energy of RH1 $p = 1$ on a (001)-oriented Si substrate, finding $\Delta E_{MS} = 5.24$ meV/atom. This is lower than the energies of all of the (001) SL's on the same substrate (except the $p = \frac{1}{2}$ zinc-blende structure, which has $\Delta E_{MS} = 4.96$ meV), which contradicts the pseudopotential results of Ciraci and Batra[13] who found that the $p = 2$ (001) SL is more stable than the $p = 1$ RH1 SL (by about 3.4 meV/atom). We will see in Sec. VI that this contradiction is not removed even when the chemical contribution to the formation energy is included.

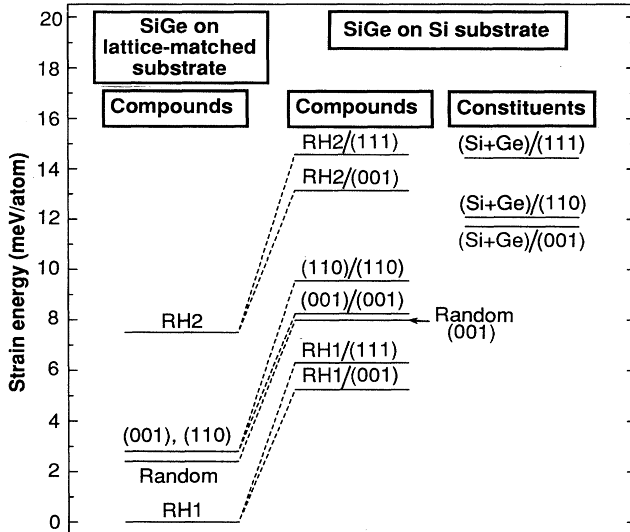

FIG. 3. Strain energy of $p = 1$ superlattices and the random alloy on lattice-matched substrates on Si substrates in various orientations (shown following the slash). The third column shows the strain energy of coherent constituents on Si substrates, demonstrating that, except for RH2 $p = 1$, the epitaxial superlattices have lower strain energy than the coherent constituents.

D. Random 50%-50% alloys on different substrates

We have calculated the microscopic strain energy of the 50%-50% *random* (*R*) $Si_{0.5}Ge_{0.5}$ alloy, using as a model the eight-atom special quasirandom structure[29] depicted in Fig. 1(c), obtaining $\Delta E_{MS}^{(R)} = 2.42$ meV/atom at $\bar{a}$ [Fig. 2(a)] and 7.98 meV/atom on a (001)-oriented Si substrate [Fig. 2(b)]. To test the quality of the SQS model for SiGe, we have calculated the strain energy of large cubic supercells with random distributions of equal numbers of Si and Ge atoms, using the AVFF model with relaxation of all cell-internal degrees of freedom as well as the lattice constant (bulk alloy) or the c/a ratio [epitaxial alloy on a (001) Si substrate]. The supercells contained either 512 or 1000 atoms, and for each we calculated the strain energy of 100 random configurations, all at 50%-50% composition. The results, including the average, minimum, and maximum energies for the 100 cases, as well as their standard deviation, are shown in Table V, and show the SQS to be a good model of the random alloy: The error in ΔE_{MS} is only 0.2 meV/atom for $a_s = \bar{a}$ and 0.02 meV/atom for $a_s = a_{Si}$, both substantially small-

TABLE V. Test of the SQS model. Here we compare the strain energies of large cubic supercells containing random distributions of equal numbers of Si and Ge atoms with the strain energy of the eight-atom SQS-8 structure. All cell-internal degrees of freedom as well as the lattice constant (bulk) or the c/a ratio (epitaxial) are fully relaxed. For the large random supercells, the average $\Delta E_{MS}^{(R)}$, minimum ΔE_{min}, and maximum ΔE_{max} energies for 100 distinct configurations, as well as their standard deviation σ, are shown. Note that the eight-atom SQS reproduces well the results of the large supercells.

Structure	$\Delta E_{MS}^{(R)}$	σ	ΔE_{min}	ΔE_{max}
	Bulk cubic alloy			
512 atoms	2.62	0.14	2.29	3.02
1000 atoms	2.61	0.10	2.33	2.80
SQS-8	2.41			
	Epitaxial alloy on (001) Si substrate			
1000 atoms	8.00	0.11	7.70	8.30
SQS-8	7.98			

er than the standard deviation of the large supercell results.

Comparison with the SL results of Figs. 2 and 3 shows that, while a number of ordered epitaxial SiGe structures on Si have lower strain energy than their strained constituents, only the ZB and RH1 $p=1$ structures also have lower strain energy than the random alloy (modeled by the SQS) of the same composition.

V. FORMALISM AND RESULTS FOR CHEMICAL ENERGIES

Having described in Sec. IV the microscopic strain energies ΔE_{MS} of the various Si/Ge SL's, we turn now to the second component of the formation enthalpy ΔH of Eq. (5), namely, the chemical energy ΔE_{chem}. We base our calculation on the technique of cluster expansion,[34,36] wherein a lattice[37] energy (here ΔE_{chem}) is represented as an expansion in a complete orthogonal set of "cluster functions,"[36] with coefficients that represent the values of that quantity for the clusters. The total chemical energy (per atom) of a configuration σ (i.e., a given arrangement of Si and Ge atoms on the N sites of a basic lattice with the diamond structure) is represented as

$$E_{\mathrm{chem}}(\sigma)=\sum_{f}^{2^N}\Pi_f(\sigma)J_f\ , \tag{16}$$

where f denotes the clusters ("figures"), J_f the chemical energy associated with cluster f, and the cluster functions $\Pi_f(\sigma)$ are products of Ising spin variables for the atoms in cluster f in configuration σ. We take the pseudospin at a site to be -1 if it is occupied by a Si atom and $+1$ if by a Ge atom. There will, in general, be a number of figures of a given type that are related by the space-group operations of the diamond structure, and this symmetry can be used to reduce the expansion to one involving only symmetry-inequivalent clusters F:

$$E_{\mathrm{chem}}(\sigma)=\sum_{F} D_F J_F \overline{\Pi}_F(\sigma)\ , \tag{17}$$

where ND_F is the number of clusters equivalent by symmetry to F, and

$$\overline{\Pi}_F(\sigma)=\frac{1}{ND_F}\sum_{f\,\mathrm{equiv}F}\Pi_f(\sigma) \tag{18}$$

is the average over the crystal of $\Pi_f(\sigma)$.

As with the strain energy and the total formation enthalpy [Eq. (1)], we wish to refer the chemical energy to the concentration-weighted average of the energies of the Si and Ge constituents. Hence, the excess chemical energy (per atom) of $\mathrm{Si}_x\mathrm{Ge}_{1-x}$ in configuration σ is given by

$$\begin{aligned}\Delta E_{\mathrm{chem}}(\sigma)&\equiv E_{\mathrm{chem}}(\sigma)\\&\quad-[xE_{\mathrm{chem}}(\mathrm{Si})+(1-x)E_{\mathrm{chem}}(\mathrm{Ge})]\\&=\sum_F D_F J_F \overline{\mathcal{P}}_F(\sigma)\ ,\end{aligned} \tag{19}$$

where

$$\overline{\mathcal{P}}_F(\sigma)=\overline{\Pi}_F(\sigma)-[x\overline{\Pi}_F(\mathrm{Si})+(1-x)\overline{\Pi}_F(\mathrm{Ge})]\ . \tag{20}$$

For the empty cluster (denoted by $F=0$) $\overline{\Pi}_0\equiv 1$ for all configurations, while for single-atom clusters (denoted by $F=1$) $\overline{\Pi}_1(\sigma)=\overline{\Pi}_1(x)=1-2x$. Also, for clusters containing an even number of atoms $\overline{\Pi}_F(\mathrm{Si})=\overline{\Pi}_F(\mathrm{Ge})=1$, and for clusters containing an odd number of atoms $-\overline{\Pi}_F(\mathrm{Si})=\overline{\Pi}_F(\mathrm{Ge})=1$. As a consequence, for all σ, $\overline{\mathcal{P}}_0(\sigma)\equiv 0$, $\overline{\mathcal{P}}_1(\sigma)\equiv 0$, $\overline{\mathcal{P}}_F(\sigma)=\overline{\Pi}_F(\sigma)-1$, for clusters containing an even number of atoms, and $\overline{\mathcal{P}}_F(\sigma)=\overline{\Pi}_F(\sigma)-(1-2x)$, for clusters containing an odd number of atoms.

It is convenient to separate the cluster-class index F into two separate indices specifying the number of atoms in the cluster (size, denoted by k), and the number of nearest-neighbor distances separating atoms in the cluster (interaction range, denoted by m). In this notation, the empty cluster has $F=(0,0)$, the single atom clusters have $F=(1,0)$, pair clusters have $F=(2,m)$ with $m\geq 1$, and so forth. Values of $\overline{\Pi}_{k,m}$ [from which $\overline{\mathcal{P}}_{k,m}$ is easily derived via Eq. (20)] are given in Table VI for a number of configurations of interest here.[38]

In general, the expansion of Eq. (19) must be truncated to some small number N_s of clusters in order to be practical. Then N_s periodic structures can be selected so that the cluster energies J_F can be obtained by solving the resulting system of equations,[35] using as input the N_s values of ΔE_{chem} obtained from first-principles calculations. The cluster energies J_F can then be used to predict ΔE_{chem} for other structures. Since $\overline{\mathcal{P}}_0(\sigma)=\overline{\mathcal{P}}_1(\sigma)\equiv 0$ for all configurations, the first nonvanishing term in the expansion is that for the nearest-neighbor-pair cluster type $F=(2,1)$. We choose to keep just two terms in the cluster expansion, corresponding to nearest-neighbor pairs and second-nearest-neighbor pairs [$F=(2,2)$]. These two cluster energies can be obtained by using just the equilibrium zinc-blende and RH1 $p=1$ structures, whose formation enthalpies equal their chemical energies, since they have $\Delta E_{\mathrm{MS}}=0$. From Table VI and Eq. (19) we have (with energies in meV/atom)

$$\begin{aligned}\Delta E_{\mathrm{chem}}^{(\mathrm{ZB})}&=-4J_{2,1}+0J_{2,2}+\cdots=9.92\ ,\\ \Delta E_{\mathrm{chem}}^{(\mathrm{RH1})}&=-3J_{2,1}-6J_{2,2}+\cdots=6.54\ ,\end{aligned} \tag{21}$$

so that the values for the cluster energies are then

$$\begin{aligned}J_{2,1}&=-2.48\ ,\\ J_{2,2}&=0.150\ .\end{aligned} \tag{22}$$

Having these J_F, we then use them to predict ΔE_{chem} for other structures, according to Eqs. (19) and (20), with the assumption that the values so derived are independent of a_s, since variations in the formation enthalpy with a_s are included in ΔE_{MS}. This is tested in Sec. VI and found to be appropriate. The results for interfacial chemical energies (I_{CE}) of SL's are given in the second column of Table IV and for ΔE_{chem} for selected structures in Table VII. Note that the small value of $I_{\mathrm{CE}}+I_{\mathrm{SR}}$ found for (001) SL's on a (001) Si substrate is consistent with the finding of Froyen *et al.*[9] that $\Delta H(p)$ is constant to within ± 1.5 meV/atom.

Other pairs of structures can be used to determine the

TABLE VI. Lattice-averaged pseudospin products $\overline{\Pi}_{k,m}$ [Eq. (18)] for several structures on the diamond lattice. $\overline{\Pi}_{2,m}$ give the pair terms for atoms separated by an mth-neighbor distance, while $\overline{\Pi}_{4,m}$ give four-body terms characterized by mth-neighbor separations. For all structures $\overline{\Pi}_{0,0}=1$, and for all structures included in the table, $\overline{\Pi}_{k,0}=0$, for k for odd. Also included is $\overline{\mathcal{P}}_{2,1}$, defined in Eq. (20). For clusters containing an even number of atoms $\overline{\Pi}_F(\mathrm{Si})=\overline{\Pi}_F(\mathrm{Ge})=1$, and for clusters containing an odd number of atoms $\overline{\Pi}_F(\mathrm{Ge})=-\overline{\Pi}_F(\mathrm{Si})=1$. Note that the $\overline{\Pi}_F$ for the SQS-8 structure closely approximate those of the random alloy, for which all are zero except $\overline{\Pi}_{0,0}$. The first row gives the degeneracies D_F of Eqs. (18) and (20).

	$\overline{\mathcal{P}}_{2,1}$	$\overline{\Pi}_{2,1}$	$\overline{\Pi}_{2,2}$	$\overline{\Pi}_{2,3}$	$\overline{\Pi}_{2,4}$	$\overline{\Pi}_{2,5}$	$\overline{\Pi}_{2,6}$	$\overline{\Pi}_{4,1}$	$\overline{\Pi}_{4,2}$
D_F	2	2	6	6	3	6	24	4	1
ZB	2	−1	1	−1	1	−1	1	−1	1
RH1 $p=1$	3/2	−1/2	0	1/2	−1	−1/2	0	1/2	−1
RH1 $p=2$	3/4	1/4	1/2	1/4	0	−1/4	0	3/4	0
RH1 $p=3$	1/2	1/2	2/3	1/2	1/3	1/6	1/3	5/6	1/3
RH2 $p=1$	1/2	1/2	0	−1/2	−1	1/2	0	−1/2	−1
RH2 $p=2$	1/4	3/4	1/2	1/4	0	1/4	0	1/4	0
RH2 $p=3$	1/6	5/6	2/3	1/2	1/3	1/2	1/3	1/2	1/3
(001) $p=1$	1	0	−1/3	0	1	0	−1/3	0	1
(001) $p=2$	1/2	1/2	1/3	1/6	1/3	−1/6	−1/3	1/2	1
(001) $p=3$	1/3	2/3	5/9	4/9	5/9	2/9	1/9	2/3	1
(110) $p=1$	1	0	−1/3	0	1	0	−1/3	0	1
(110) $p=2$	1/2	1/2	0	−1/6	−1/3	−1/6	0	−1/2	−1
SQS-8	1	0	0	0	−1/3	0	0	0	−1

interaction parameters by simply solving Eq. (5) for ΔE_{chem}, using the pseudopotential result for ΔH and the AVFF result for ΔE_{MS}. Several of these (e.g., ZB and RH2 or RH1 and RH2) give results of comparable quality to those in Eq. (22). The rapid decay of chemical interactions with distance ($J_{2,1}/J_{2,2}\sim 16$) and the fact that $J_{k,m}$ can be extracted from different sets of structures with similar results suggests that the cluster expansion for ΔE_{chem} converges rapidly (though it is not yet fully converged with just two terms,[39] as is evidenced by the fact that the error in $\Delta H_{\mathrm{model}}$ is greater than the error in the AVFF results). This rate of convergence is greater than that found[34] for cluster expansions of the *total* formation enthalpy in fcc-based (e.g., pseudobinary) systems. We believe that it will generally be true that, for lattice-mismatched systems, cluster expansions of ΔE_{chem} converge faster than those for ΔH. This probably reflects the fact that the equivalence classes of clusters (denoted F) are determined via the diamond space group (that being the symmetry of the underlying *undistorted* lattice upon which the alloy is built), but some of these classes split upon relaxation of individual structures. In our model, the symmetry-breaking interactions are handled via the AVFF, in which no symmetry-based cluster equivalence is assumed, while the symmetry-preserving chemical interactions are handled via a rapidly convergent cluster expansion.

To demonstrate the effects of relaxation on the convergence of cluster expansions of total formation enthalpies, we have generated expansions (Table VIII) based on the pseudopotential results of de Gironcoli, Baroni, and Giannozzi,[40] who used a plane-wave cutoff energy of 12 Ry and a **k**-point sampling equivalent to two special points in the irreducible part of the diamond Brillouin

TABLE VII. Component and total formation enthalpies for a number of SiGe systems. ΔE_{chem} is the prediction of our cluster expansion [Eqs. (19)–(22)] and is independent of a_s, ΔE_{MS} is the AVFF-predicted microscopic strain energy [Eq. (9)], and $\Delta H_{\mathrm{model}}$ is the model-predicted value $\Delta E_{\mathrm{MS}}+\Delta E_{\mathrm{chem}}$ [right-hand side of Eq. (5)]. ΔH_{ps} is the directly calculated pseudopotential result [left-hand side of Eq. (5)]. The random alloy values are those from the SQS-8 model. The results for a_{Si} are for the (001) surface. Parenthesized values for $\Delta H_{\mathrm{model}}$ are those for structures used as input to the cluster expansion for ΔE_{chem}; all others are predicted by the model. The accuracy of the model can be assessed by comparing these other values of $\Delta H_{\mathrm{model}}$ to ΔH_{ps}.

			$a_s=a_{\mathrm{SL}}$			$a_s=a_{\mathrm{Si}}$	
	ΔE_{chem}	ΔE_{MS}	$\Delta H_{\mathrm{model}}$	ΔH_{ps}	ΔE_{MS}	$\Delta H_{\mathrm{model}}$	ΔH_{ps}
ZB	9.92	0.00	(9.9)	9.9	4.96	14.9	14.9
RH1 $p=1$	6.54	0.00	(6.5)	6.5	5.24	11.8	11.7
RH2 $p=1$	1.58	7.50	9.1	9.2	13.12	14.7	14.9
(001) $p=1$	3.76	2.80	6.6	6.8	8.24	12.0	
(001) $p=2$	1.88	4.35	6.2		9.97	11.9	
Random	4.06	2.41	6.5	6.1	7.98	12.0	11.5
Si+Ge	0.0	0.00	0.0	0.0	11.70	11.7	11.7

TABLE VIII. Results of cluster expansions based on the pseudopotential (PS) results of Ref. 40 for 11 SiGe structures in both the unrelaxed (ideal atomic positions) and relaxed configurations. Superlattices are denoted by the orientation **G** (or RHn for the [111] SL's), in parentheses, the numbers of Si and Ge monolayers, respectively. Values for those structures used as input for the determination of the cluster energies are enclosed in parentheses; the rest are predictions and are to be compared with the direct pseudopotential results. The unrelaxed systems are reproduced well by a three-term cluster expansion including only J_0, $J_{2,1}$, and $J_{2,2}$, whereas the error in a similar three-term cluster expansion of the relaxed systems is far larger. In order to achieve comparable convergence in the cluster expansion for the relaxed systems, it is necessary to continue the expansion to six terms, including J_0, $J_{2,1}$, $J_{2,2}$, $J_{2,5}$, $J_{2,6}$, and $J_{2,7}$. The cluster-expansion predictions for the random 50%-50% alloy are also shown. Both the three-term value for the unrelaxed alloy and the seven-term value for the relaxed alloy are in good agreement with the best predictions shown in Fig. 1 of Ref. 40, and are in excellent agreement with the most-converged cluster expansions we can generate from these 11 structures (−4.2 and −8.1 meV/atom, respectively), whereas the three-term prediction for the relaxed alloy is clearly under converged.

	Unrelaxed		Relaxed		
	PS[a]	Three terms	PS[a]	Three terms	Six terms
ZB	−6.5	(−6.5)	−6.5	(−6.5)	(−6.5)
[001] (2,2)	−4.6	−4.4	−9.7	−10.7	−9.7
[001] (3,1)	−3.9	−3.9	−6.4	−7.8	−6.5
[001] (1,3)	−3.9	−3.9	−6.5	−7.8	(−6.5)
[001] (3,3)	−3.2	−3.1	−9.5	−8.3	(−9.5)
[110] (2,2)	−2.7	−2.6	−10.7	−8.5	(−10.7)
[110] (3,1)	−2.5	(−2.5)	−7.8	(−7.8)	(−7.8)
[110] (1,3)	−2.5	−2.5	−7.9	−7.8	−7.8
RH1 (2,2)	−5.7	(−5.7)	−10.0	(−10.0)	−9.9
RH2 (2,2)	−2.5	−2.6	−6.3	−8.5	−6.3
RH3 (3,3)	−3.0	−2.9	−7.9	−7.3	(−7.9)
Random		−4.2		−9.3	−8.1

[a]From Ref. 40.

zone. Their results for formation enthalpies of eight unrelaxed (ideal) structures, taken with respect to the binaries at $a=\bar{a}$, can be reproduced to within 0.2 meV/atom with a cluster expansion including only J_0, $J_{2,1}$, and $J_{2,2}$, with interactions determined from three other structures of their total set of 11. However, using their analogous results for relaxed structures the maximum error jumps to nearly 2.2 meV/atom, for the same structure-interaction combination. In order to reduce the error to a level comparable to that for the unrelaxed structures, one needs to include up to seventh-nearest-neighbor pairs ($J_{2,7}$) (requiring six structures as input and leaving only five to serve as the measure of convergence). Thus we see that the cluster expansion of ΔE_{chem} has a convergence rate comparable to that of the cluster expansion for total formation enthalpies of *unrelaxed* structures, which is considerably faster than that for *relaxed* structures.

Note that the analysis of ΔE_{chem} given by Koiller and Robbins,[14] based on (nearest-neighbor) "bond energies" alone, is equivalent to retaining just the single term $J_{2,1}$ in the cluster expansion.[41] We find that considerable improvement is afforded by the inclusion of the $J_{2,2}$ term. Nevertheless, the rough proportionality of ΔE_{chem} (Table VII) to $\bar{\mathcal{P}}_{2,1}$ (Table VI) is consistent with the expected dominance of the nearest-neighbor-pair interactions.

VI. TOTAL FORMATION ENTHALPIES

Combining the chemical energy with the microscopic strain energy $\Delta E_{\text{MS}}^{(\alpha)}$ then gives, according to Eq. (5), the total formation enthalpy $\Delta H_{\text{model}}^{(\alpha)}$ predicted by our model. This model energy and its components are summarized in Table VII both for equilibrium "free floating" SL's ($a_s=a_{\text{SL}}$) and for SL's on a (001) Si substrate. To test the model we present in Table VII the results of our direct first-principles calculations (denoted $\Delta H_{\text{ps}}^{(\alpha)}$) where available. Comparison of $\Delta H_{\text{model}}^{(\alpha)}$ with $\Delta H_{\text{ps}}^{(\alpha)}$ for the six systems *not used* to extract ΔE_{chem} shows that the model captures all trends underlying the directly calculated formation enthalpies to within better than 0.5 meV/atom. In view of this relatively small residual error, we can use our model to predict $\Delta H(p,\mathbf{G},a_s)$ for SL's that are too large to calculate directly from first principles. This is done in Table IX.

Tables VII and VIII demonstrate a number of features.

(1) The chemical energy constitutes a significant fraction of the total formation enthalpy: e.g., 60% for the random alloy, 20% for RH2, and 100% for ZB and RH1. For SL's, the trend in ΔE_{chem} with p usually opposes the trend in ΔE_{MS} (the interface energies have opposite signs), so that the trend in ΔH is not evident from consideration of either ΔE_{MS} or ΔE_{chem} alone.

(2) The model-predicted formation enthalpy of the bulk random alloy, 6.5 meV/atom, is close to the directly calculated pseudopotential value of 6.1 meV/atom. For comparison, we note that Kelires and Tersoff[42] found, using an empirical potential, $\Delta H(\text{random})=7.3$ meV/atom, while Qteish and Resta[43] found from their first-principles statistical model 11.3 meV/atom. Stringfellow[44] found experimentally 6.5 meV/atom. We note also that the cal-

culations of Qteish and Resta[43] place the random alloy 2.0 meV/atom higher in energy than the zinc-blende structure, whereas our first-principles results place it 3.8 meV/atom below ZB. This discrepancy may arise from their use of only partial relaxation of the component structures used in their random alloy model or from the difference in cutoff energies (12 Ry used in Ref. 43 versus 20 Ry used here) and **k**-point sampling (the equivalent of two special points in the irreducible wedge of the diamond Brillouin zone used in Ref. 43 versus ten used here).[45]

(3) The formation enthalpies of the bulk random alloy and bulk RH1 $p=1$ are quite close, suggesting that the unstrained random alloy is essentially equal in stability to unstrained RH1 at zero temperature, and would thus be favored over RH1 at finite temperature because of the larger configurational entropy contribution to the free energy. The epitaxially strained RH1 structure is also essentially degenerate with the random alloy. One could estimate corrections due to the underestimation of bond lengths and Si/Ge lattice mismatch by the first-principles calculations as follows. If we use in the AVFF for RH1 $p=1$ on (001) Si and SQS on (001) Si, the experimental (rather than pseudopotential) bond lengths used by Koiller and Robbins,[14] the ΔE_{MS} increase by 4.26 and 5.49 meV/atom, respectively, giving total formation enthalpies of 16.0 and 17.5 meV/atom, respectively. The difference of 1.5 meV/atom is still far too small to account for the transition temperature observed by Ourmazd and Bean.[18]

(4) RH1 $p=1$ on (001) Si is essentially degenerate with the (001) $p=2$ SL on (001) Si, still in contrast to the results of Ciraci and Batra,[13] who found RH1 to be higher by about 3.4 meV/atom. This reflects some combination

TABLE IX. Model-predicted component and total formation enthalpies for a number of SiGe superlattices. ΔE_{chem} is the prediction of our cluster expansion [Eqs. (19)–(22)] and is common to both $a_s=a_{\mathrm{SL}}$ and $a_s=a_{\mathrm{Si}}$, ΔE_{MS} is the AVFF-predicted microscopic strain energy [Eq. (9)], and $\Delta H_{\mathrm{model}}$ is the sum $\Delta E_{\mathrm{MS}}+\Delta E_{\mathrm{chem}}$ [right-hand side of Eq. (5)]. The random alloy values are those from the SQS-8 model.

		$a_s=\bar{a}$		$a_s=a_{\mathrm{Si}}$	
	ΔE_{chem}	ΔE_{MS}	$\Delta H_{\mathrm{model}}$	ΔE_{MS}	$\Delta H_{\mathrm{model}}$
(001) superlattices on (001) substrates					
ZB	9.92	0.06	9.98	4.96	14.88
$p=1$	3.76	2.83	6.59	8.24	12.00
$p=2$	1.88	4.37	6.24	9.97	11.85
$p=3$	1.25	4.87	6.13	10.55	11.80
$p=10$	0.38	5.59	5.96	11.36	11.73
$p=\infty$	0.00	5.89	5.89	11.70	11.70
(110) superlattices on (110) substrates					
$p=1$	3.76	2.81	6.57	9.54	13.30
$p=2$	1.58	4.53	6.10	10.68	12.26
$p=3$	1.05	5.49	6.55	11.21	12.26
$p=10$	0.32	6.58	6.90	11.81	12.13
$p=\infty$	0.00	7.05	7.05	12.07	12.07
RH1 superlattices on (111) substrates					
$p=1$	6.54	0.07	6.61	6.29	12.83
$p=2$	3.27	3.78	7.05	10.37	13.64
$p=3$	2.18	5.01	7.19	11.72	13.90
$p=10$	0.65	6.73	7.39	13.62	14.27
$p=\infty$	0.00	7.47	7.47	14.43	14.43
RH2 superlattices on (111) substrates					
$p=1$	1.58	7.51	9.09	14.56	16.14
$p=2$	0.79	7.49	8.28	14.50	15.29
$p=3$	0.53	7.49	8.01	14.47	15.00
$p=10$	0.16	7.48	7.63	14.44	14.60
$p=\infty$	0.00	7.47	7.47	14.43	14.43
Random alloy on (001) substrates					
Random	4.06	2.42	6.48	7.98	12.04
Rhombohedral $p=1$ superlattices on (001) substrates					
RH1	6.54	0.04	6.58	5.24	11.78
RH2	1.58	7.51	9.09	13.12	14.70

of incomplete relaxation of RH1 by Ciraci and Batra, the smaller basis set used by them, and residual errors in our model calculation. A direct first-principles calculation of RH1 on a (001) Si substrate yields a formation enthalpy of 11.7 meV/atom, only 0.1 meV/atom below our estimate given above (reflecting the residual errors in our model calculation). Since the use of a smaller plane-wave basis set appears to increase the lattice mismatch between Si and Ge (see, e.g., Ref. 9), and this would increase the strain energy of the $p=2$ (001) SL more than that of $p=1$ RH1 (since the former is more highly strained), we must conclude then that the bulk of the discrepancy between our results and those of Ciraci and Batra[13] is due to their incomplete relaxation of the RH1 structure, a conclusion also voiced by Koiller and Robbins[14] (though in their case it was based entirely on elastic energies).

(5) Epitaxial RH1 $p=1$ on (001) Si has an epitaxial formation enthalpy [Eq. (15)] $\delta H_{\rm ps} \approx 0$. This differs from the calculations of Martins and Zunger,[12] who found $\delta H_{\rm ps} \approx -2$ meV/atom, probably because of the difference in $\mathbf{k}$-point sampling (see Sec. III A). On a (001) Ge substrate, our model gives $\delta H = 1.1$ meV/atom (i.e., epitaxially unstable), in contrast to the model results of Mäder, von Känel and Baldereschi,[46] who find RH1 $p=1$ to be epitaxially stable on (001) Ge.

(6) The RH2 $p=1$ structure, having $\Delta H = 9.2$ meV/atom and $\delta H = +3.2$ meV/atom, is unquestionably higher in energy than either the RH1 $p=1$ structure or the random alloy. It is clear also that this is so because its much higher strain energy overwhelms the lower chemical energy. Thus, we conclude that the RH2 $p=1$ ordering seen in bulk (unstrained) SiGe by LeGoues, Kesan, and Iyer[19] is not mandated by bulk thermodynamics (through the difference in chemical energy) as they originally suggested.

VII. OTHER INTERFACIAL INTERACTIONS

Calculations of the energy of a SL on a substrate with a_s different from $a_{\rm SL}$ (the natural SL lattice constant in the substrate plane) have traditionally [e.g., Sec. IV and Fig. 2(b)] been done by imposing a biaxial strain on the SL, thus enforcing *lattice*[47] registry, i.e., confining the lattice points of the SL to be in registry with their analogs in the substrate. This constraint, which we term a "virtual substrate," does not account for other interactions with the substrate through the requirement of *atomic* registry at the substrate/SL interface (relevant when there are more atoms than lattice points in the substrate interface plane of the SL), relaxation of the atoms near the interface, and charge transfer at the interface. The last two of these depend on the identities of the atoms on both sides of the interface, including those of the substrate. For example, in the virtual substrate approach, a Ge, GaAs, or ZnSe substrate would have the same effect on films grown on them, insofar as these substrates have similar lattice constants. Here we examine the microscopic interactions at a (001) Si/SiGe interface, such as that between an epitaxial SL film and the Si substrate on which it is deposited. This will allow us to determine under what circumstances the usual omission of all but the biaxial strain component of that interaction is justified, as well as to investigate the possibility that interface stabilization could have an effect on spontaneous ordering of SiGe alloys, such as has been observed by Ourmazd and Bean.[18] In addition, we will consider some other types of (001) interfaces with SiGe in order to look for other possibilities for stabilization of particle SiGe phases.

Our model system consists of a sequence of (001)-oriented $(\mathrm{Si}_4)_q/(\mathrm{Si}_2\mathrm{Ge}_2)_q$ SL's, with the SiGe layers in the RH1 ($p=1$), RH2 ($p=1$), SQS-8, and (001) SL (with maximal $p=q/2$) structures (the latter serving to model the most completely phase-separated state possible within the $2q$ SiGe layers). A virtual (001) Si substrate constraint is applied to these SL's in order to include the biaxial-strain effect of a very thick Si substrate. For large q the Si/SiGe interface within the SL then provides a model of an isolated (001) Si/SiGe interface, such as that between a relatively thick SiGe film and a thick *real* Si substrate, including atomic registry at the interface, full relaxation of the atomic positions of both the film and the "substrate" (Si layers), and chemical interactions. In addition, for finite q (≈ 28) the results give a direct indication of the effect of the interfaces on the energies of Si/SiGe SL's similar to those investigated by Ourmazd and Bean.[18] Since the "constituents" of this system are Si and SiGe, there is a nonzero contribution to the chemical energy from the SiGe constituent even in the $q \to \infty$ limit. In addition, both the strain and chemical energies depend on the state of order α of the SiGe layers. Thus, Eq. (6) must be modified in this case to read

$$\Delta H(q,\mathbf{G},a_s,\alpha) = \Delta E_{\rm CS}(\mathbf{G},a_s,\alpha) + \Delta E_{\rm CC}(\alpha) + \frac{1}{2p}[I_{\rm SR}(q,\mathbf{G},a_s,\alpha) + I_{\rm CE}(q,\mathbf{G},\alpha)] , \tag{23}$$

where $\Delta E_{\rm CC}$ denotes the constituent (Si and SiGe) chemical energy. The number of double layers q is taken to be a multiple of four, which allows an integral number of complete primitive unit cells of all the SiGe structures to be included in the SL, as well as being sufficient to limit small-q interface-interface interaction effects that contribute to substantial small-q dependence of the interface energies. The strain-only results are shown in Fig. 4, and the complete results for the interface and constituent energies [derived by fitting the large-q formation energies to Eq. (23)] are shown in Table X, from which we note the following.

In each case there are two (pairs of) variants (denoted "a" and "b"), depending on the orientation of the SiGe structure relative to the Si layer. The a variants can be characterized as having uniform (3 Si and 1 Ge) coordination of the Si atoms at the Si side of the interface, and mixed coordination (half of the atoms coordinated by 4 Si and half coordinated by 2 Si and 2 Ge) of the Si and Ge atoms at the SiGe side of the interface. For the b variants the pattern is reversed, with uniform coordination at the SiGe side and mixed coordination at the Si side of the interface. Since the Si layer is largely unstrained (except

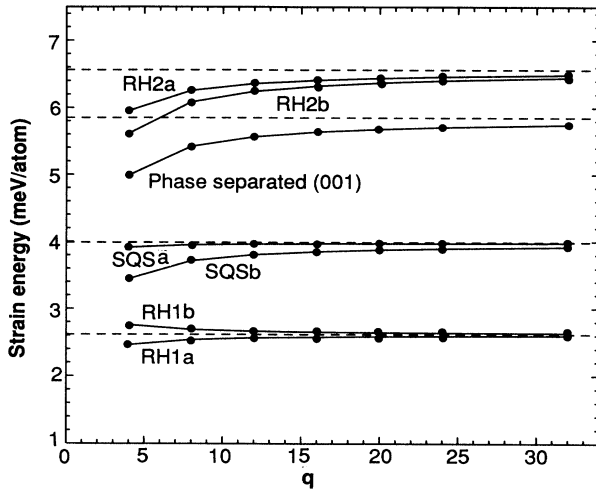

FIG. 4. Strain energy of [001]-oriented $(Si_2)_q/(SiGe)_q$ superlattices on a [001]-oriented Si substrate. The variants a and b arise from symmetry breaking of the SiGe structures caused by the presence of Si/SiGe interfaces and are described in the text. The curve labeled "phase-separated" has maximally phase-separated (along [001]) SiGe alternating with Si.

near the interface), the strain energy per atom of the SiGe layer alone is essentially twice that shown in Fig. 4. A similar statement applies to the chemical energy ΔE_{CC} shown in Table X. In the $q \to \infty$ limit, the variants become degenerate, and the formation enthalpy per atom of SiGe is just the result obtained from a calculation of SiGe on a virtual (001) Si substrate (Fig. 2). The total energies of conventional virtual-substrate calculations are recovered to within 1% by $q=24$. For all q, the RH1a variant has slightly lower strain energy than the RH1b variant, though the largest splitting shown in Fig. 4, for $q=4$, is less than 0.3 meV/atom, only about 1% of kT at room temperature.

The variants are energetically distinguished only by their interface energies, and the strain (SR) and chemical (CE) contributions to these are always of opposite sign, so that their sum is generally smaller in magnitude than either contribution. Hence, the distinction between the variants is smaller in the total interface energies than in either contribution. We note the exceptionally large (001) total interface energies of RH2a and RH2b. A consequence of this is that in thin layers of SiGe on (001) Si, the energy difference between RH1 and RH2 will be reduced. This is especially evident for very small q, as is shown in Table XI. Indeed, for $q=1$ we find that the total formation energy of the RH2a variant is very slightly lower than that of RH1a, while the two b variants are degenerate by virtue of being structurally equivalent. However, for $q<4$ the identities of the SiGe phases are not well defined because the slab does not contain complete unit cells of them.

We conclude that for sufficiently thick (large q) films substrate interface effects are negligible in these structures when grown on (001) substrates, and will not alter the conclusions drawn from calculations based on the use of virtual substrates. Indeed, for the systems considered in Fig. 4 and Table XI, the $q=4$ energy order is exactly the same as that in the $q \to \infty$ (virtual substrate) limit. We also conclude that well-separated Si/SiGe interfaces cannot help to explain the discrepancy between calculated order-disorder transition temperatures and that observed by Ourmazd and Bean[18] in a structure similar to our $q=28$ Si/SiGe SL.

It is useful to consider under what circumstances the film-substrate interface interactions omitted by the common use of a virtual substrate might become more important. In particular, we consider the fact that the *lattice* registry imposed by a virtual substrate does not necessarily imply *atomic* registry at the interface. This is of no concern when lattice registry implies atomic registry, as is the case for SL's grown on "native" substrates, i.e., substrates whose surface normal $\mathbf{G}_s$ is parallel (or nearly so) to the SL stacking direction $\mathbf{G}$. However, for SL's grown on "foreign" substrates, i.e., with $\mathbf{G}_s$ not parallel to $\mathbf{G}$, such as (110) or (111) SiGe SL's grown on (001) Si substrates, the number of interface atoms not lying at lat-

TABLE X. Interfacial chemical (I_{CE}), strain-relief (I_{SR}), and total (I) energies (meV/primitive-cell interface) in the $q \to \infty$ limit (i.e., isolated interfaces), constituent chemical energies ΔE_{CC} (meV/atom), and constituent strain energies ΔE_{CS} (meV/atom) for various [001]-oriented A/B SL's on a (001) Si substrate. Here A consists of q double layers of Si, Ge, or SiGe in one of the phases RH1 or RH2, and B consists of q double layers of SiGe in one of the phases RH1, RH2, SQS-8 (quasirandom), or phase separated along [001] with $p=q/2$ (PS). Hence, one or both of the "constituents" contributing to ΔE_{CC} and ΔE_{CS} here is SiGe. The interface unit cell is 2×1, and all interfaces are (001) oriented. Note that there is no a/b variant distinction for the Si/Ge interface (Si/PS) or the RH1/RH2 interface. All rhombohedral structures included here are the $p=1$ SL. APB denotes a (001)-oriented antiphase boundary.

Interface	$I_{CE}^{(a)}(\infty)$	$I_{SR}^{(a)}(\infty)$	$I^{(a)}(\infty)$	$I_{CE}^{(b)}(\infty)$	$I_{SR}^{(b)}(\infty)$	$I^{(b)}(\infty)$	ΔE_{CC}	ΔE_{CS}
Si/RH1	3.76	−2.49	1.27	−1.20	2.27	1.07	3.27	2.62
Si/RH2	3.76	−9.81	−6.05	8.72	−15.28	−6.56	0.79	6.56
Si/SQS-8	3.76	−1.16	2.60	8.72	−8.74	−0.02	2.03	3.99
Si/PS	15.03	−13.84	1.20				0.00	5.85
Ge/RH1	3.76	−3.38	0.38	−1.20	2.85	1.64	3.27	14.32
Ge/RH2	3.76	−10.14	−6.38	8.72	−14.66	−5.94	0.79	18.27
RH1 APB	0.00	1.19	1.19	−9.92	11.95	2.03	6.54	5.24
RH2 APB	0.00	−12.57	−12.57	9.92	−23.20	−13.28	1.58	13.12
RH1/RH2	0.00	−2.78	−2.78				4.06	9.18

tice points increases linearly with the repeat period ($4p$) of the SL. Consequently, we expect that there would be a significant p dependence of the omitted atomic-registry contribution to the film-substrate interface energy of $(Si_2)_p/(Ge_2)_p$ SL's grown on foreign substrates [hence our omission of them from the results of Fig. 2(b)]. And we expect that for large p the film thickness (q in our model structure) required to make the film-substrate interface energy unimportant could become large. Another circumstance in which the film-substrate interface interaction can be expected to become important is when the film thickness is small enough that interactions between the film-substrate interface and the top surface of the film become substantial. For example, in the small-q limit of our model SL structure, where there is no real top surface, but just another Si/SiGe interface, we observe substantial variations in the strain energies as a function of q (Table XI).

Since we have seen that the (001) Si/SiGe interface can be stabilizing (for RH2 $p=1$), it would be of some interest to consider other interfaces to see whether they might also be stabilizing. By calculating the energies of Ge/SiGe SL's on a (001) Si substrate, we obtain the Ge/SiGe interface (and constituent) energies shown in Table X. These are generally quite similar to those for Si/SiGe, with the Ge/RH1 interface energies being positive, and the Ge/RH2 interface energies being negative. Similarly, we have calculated the energies of SiGe/SiGe SL's on (001) Si to obtain the interface energies of (001) antiphase boundaries (APB's) in RH1 $p=1$ and RH2 $p=1$ and of the RH1/RH2 (both $p=1$) (001) interface. These results are also shown in Table X. The energy of the (001) RH2 $p=1$ APB is much more stabilizing than any of the others. A natural question to ask then is whether a high density of these APB's could make the RH2 $p=1$ structure epitaxially stable on (001) Si. A simple calculation based on Eq. (23) (but ignoring the q dependence of the interface energy, i.e., ignoring interface-interface interactions) suggests that for $q=1$ (one double layer of RH2 $p=1$ followed by a similar, but phase-reversed, double layer) epitaxial stability should be achieved. The predicted formation energy is 11.4 meV/atom. To check this, we calculated such a structure with our model, and found that its formation energy (12.0 meV/atom, reduced from 14.7 meV/atom without APB's is still higher than that of the coherent constituents (11.7 meV/atom) because of interaction between the closely spaced interfaces. Thus, even in this extreme case, the interfaces do not cause RH2 $p=1$ to become epitaxially stable.

VIII. Si/Ge INTERFACE STRUCTURE

Up to now our discussion of interfaces has assumed an abrupt transition between Si and Ge, or between two

TABLE XI. Small-q and $q\rightarrow\infty$ results for $(Si_4)_q/(Si_2Ge_2)_q$ SL's on a (001) Si substrate. ΔH_{model} is the model-predicted value obtained by adding ΔE_{MS} and ΔE_{chem} [right-hand side of Eq. (5)]. ΔE_{chem} [Eq. (19)] is common to both $a_s=\bar{a}$ and $a_s=a_{\text{Si}}$.

		a variants			b variants	
	ΔE_{chem}	ΔE_{MS}	ΔH_{model}	ΔE_{chem}	ΔE_{MS}	ΔH_{model}
			RH1 $p=1$ SiGe layers			
$q=1$	4.21	1.96	6.17	2.97	3.05	6.02
$q=2$	3.74	2.29	6.03	3.12	2.84	5.96
$q=3$	3.58	2.41	5.99	3.17	2.80	5.97
$q=4$	3.50	2.46	5.96	3.19	2.76	5.95
$q=\infty$	3.27	2.62	5.89	3.27	2.62	5.89
			RH2 $p=1$ SiGe layers			
$q=1$	1.73	4.37	6.10	2.97	3.05	6.02
$q=2$	2.50	3.88	6.38	1.88	4.82	6.70
$q=3$	1.10	5.74	6.85	1.52	5.29	6.80
$q=4$	1.02	5.95	6.98	1.33	5.61	6.95
$q=\infty$	0.79	6.56	7.35	0.79	6.56	7.35
			SQS-8 SiGe layers			
$q=1$	1.73	4.37	6.10	2.97	3.05	6.02
$q=2$	2.50	3.88	6.38	3.12	2.84	5.96
$q=3$	1.93	4.30	6.23	2.34	3.87	6.21
$q=4$	2.26	3.91	6.18	2.57	3.44	6.02
$q=\infty$	2.03	3.99	6.02	2.03	3.99	6.02
			Phase-separated $Si_{0.75}Ge_{0.25}$			
$q=1$	4.36	2.42	6.78			
$q=2$	1.88	4.12	6.00			
$q=3$	1.25	4.70	5.95			
$q=4$	0.94	4.99	5.93			
$q=\infty$	0.00	5.85	5.85			

phases. There is, however, the possibility of interdiffusion at such interfaces, resulting in a different phase in the region of the (now finite) interface. Mäder, von Känel and Baldereschi[46] have recently studied this possibility using a harmonic VFF model together with the equivalent of a single-term cluster expansion for the chemical energy.[48] They pointed out that the dependence of the interface energy on interface separation (indexed by q in the model of Sec. VII, for example) could result in (1) stability of a finite-width ordered region sandwiched between Si and Ge even though the bulk phase is epitaxially unstable or (2) inability of an interdiffused ordered region to form at low temperature because of instability of thin layers, even though the bulk phase is epitaxially stable.

Comparison of our formation energies of the RH1 $p=1$, RH2 $p=1$, and SQS-8 phases on (001) substrates with the corresponding $p\rightarrow\infty$ (001) SL formation energy (Table IX) shows that none of them is epitaxially stable on a (001) substrate with either $a_s=\bar{a}$ or $a_s=a_{Si}$. Thus, we would not expect interdiffusion of Si and Ge into one of these phases at a (001) Si/Ge interface, unless the formation of SiGe/Si and SiGe/Ge interfaces stabilizes one or more of them. From Table X we see that for sufficiently widely spaced interfaces (i.e., ignoring interface-interface interaction) only the RH2 $p=1$ and the SQS-8b structures have (001) interfaces with Si and Ge that are more stable than the abrupt (001) Si/Ge interface (while epitaxially constrained to a Si substrate). Only interface-interface interaction (requiring thin layers between interfaces) or a change of substrate could alter this picture and produce epitaxial stability of one of the ordered phases in a thin region.

To test these possibilities, we have applied our energy model to a sequence of superlattices consisting of (001)-stacked layers Si/SiGe/Ge/SiGe, with a (fixed) total of 64 double layers per period, q of these devoted to each of the SiGe sections. Thus $q=0$ corresponds to two abrupt Si/Ge interfaces per period, and $q=32$ corresponds to pure SiGe with no interfaces. SL's with $0<q<32$ have two Si/SiGe and two Ge/SiGe interfaces per period. The SiGe sections were constructed with RH1 $p=1$, RH2 $p=1$, or SQS-8 ordering, and the entire assembly was subjected to a (001) virtual substrate constraint. The substrate lattice constants used were a_{Si}, $\bar{a}$, and a_{Ge}. The results for the a_{Si} substrate are presented in Table XII, and show *no tendency for thin ordered layers to be more stable than the abrupt interface.* Our results for $\bar{a}$ and a_{Ge} substrates also show the abrupt interface to be more stable than thin ordered regions in any of these three phases.[49]

While we have obviously not considered all possible phases for the SiGe regions, and have not considered nonabrupt Si/SiGe and Ge/SiGe interfaces, it appears to be generally true that the instability of the ordered SiGe phases is not overcome by interface effects in the (001) orientation, and the abrupt (001) Si/Ge interface is energetically favored.

IX. SUMMARY AND DISCUSSION OF SPONTANEOUS ORDERING

A. Summary of our results

We have decomposed the formation enthalpy of $(Si_2)_p/(Ge_2)_p$ SL's into bulk and interfacial terms [Eq. (6)], where the bulk part is just the purely elastic energy of the constituents (CS) strained to match the lattice constant a_s, and the interfacial part is composed of strain-relief (SR) and chemical energy (CE) terms. The strain-related parts ΔE_{CS} and I_{SR} are calculated via an anharmonic valence-force-field model, with force constants and equilibrium bond lengths determined from first-principles pseudopotential calculations, and the chemical-energy-related part I_{CE} is calculated with a two-term cluster ex-

TABLE XII. Results for $(Si_4)_{32-q}/(Si_2Ge_2)_q/(Ge_4)_{32-q}/(Si_2Ge_2)_q$ SL's on a (001) Si substrate. ΔH_{model} is the model-predicted value obtained by adding ΔE_{MS} and ΔE_{chem} [right-hand side of Eq. (5)]. The interface unit cell is 2×1. For $q=0$ (abrupt interface) and $q=32$ (no interface), there is no a/b variant distinction.

		a variants			b variants	
	ΔE_{chem}	ΔE_{MS}	ΔH_{model}	ΔE_{chem}	E_{MS}	ΔH_{model}
			Abrupt Si/Ge interface			
$q=0$	0.12	11.60	11.71			
			RH1 $p=1$ SiGe layers			
$q=1$	0.26	11.45	11.71	0.19	11.55	11.74
$q=2$	0.47	11.25	11.72	0.39	11.34	11.73
$q=3$	0.67	11.05	11.72	0.59	11.14	11.73
$q=4$	0.88	10.85	11.73	0.80	10.93	11.73
$q=32$	6.54	5.24	11.78			
			RH2 $p=1$ SiGe layers			
$q=1$	0.11	11.65	11.75	0.19	11.55	11.74
$q=2$	0.16	11.65	11.80	0.23	11.57	11.80
$q=3$	0.21	11.69	11.89	0.28	11.61	11.89
$q=4$	0.26	11.73	11.98	0.33	11.65	11.98
$q=32$	1.58	13.12	14.70			

pansion based on first-principles results for the two topologically unconstrained structures ZB and RH1 $p=1$. Values for these quantities are given in Tables IV and VIII, the latter containing also directly calculated first-principles results for selected structures. The epitaxial formation enthalpy $\delta H(p,\mathbf{G},a_s)$ (taken with respect to constituents coherent with the substrate) is given by Eq. (15), and its sign depends on the signs and magnitudes of its two components, both of which are purely interfacial in nature.

Considering only the strain energy of $(\mathrm{Si}_2)_p/(\mathrm{Ge}_2)_p$ SL's, we found that (i) for *long-period* SL's, the stability sequence is like that in lattice-mismatched pseudobinary III-V SL's:[17] $(001)>(110)>(111)$, reflecting the orientation-dependent constituent strain ΔE_{CS}; yet (ii) for *short-period* SL's the interfacial strain relaxation I_{SR} favors the RH1 form of the (111) SL over (001) and (110), while the RH2 form has the highest energy; (iii) only the ZB and $p=1$ RH1 structures have lower strain energy that the random alloy, and this is so both for $a_s=\bar{a}$ and $a_s=a_{\mathrm{Si}}$; and (iv) straining the SL coherently on a substrate leads to an epitaxial stabilization [largest for (111)] through the strain that would be imposed on coherent, phase-separated constituents, thus hindering phase separation.

When the chemical energy is included, the picture changes somewhat: (i) The RH1 form is no longer favored over the (001) and (110) SL's for small p, being nearly degenerate with them at $p=1$, and higher for $p>1$. (ii) The (110) SL is slightly lower in energy at $p=2$ than the (001) SL, and is higher thereafter. (iii) The sign of the interface energy in the (001) SL is now small and positive, whereas it was substantial and negative in the strain-only picture. This makes the (001) SL epitaxially unstable on both $\bar{a}$ and a_{Si} (001) substrates, whereas it is epitaxially stable in the strain-only picture. (iv) The sign of the interface energy of the (110) SL becomes positive on a (110) a_{Si} substrate, thus making it epitaxially unstable, whereas it is epitaxially stable on an $\bar{a}$ substrate, and in the strain-only picture it is epitaxially stable on both substrates.

Consideration of the full range of interactions at a film-substrate interface (Sec. VII) showed that (i) the interface between a (111) $(\mathrm{Si}_2)/(\mathrm{Ge}_2)$ SL and a (001)-oriented Si substrate partially breaks the energy degeneracy between the four different $\langle 111\rangle$ SL orientations, slightly stabilizing one pair of variants of the SL relative to the other pair; (ii) the film-substrate interface energy can safely be neglected for sufficiently thick films provided that the requirement of *atomic* registry at the interface is not substantially violated for the particular crystal structure of the film.

For several types of isolated Si/SiGe, Ge/SiGe, and SiGe/SiGe interfaces we found negative (stabilizing) interface energies, particularly those in which RH2 $p=1$ was one of the constituents. The most stable among those we investigated is the (001) antiphase boundary in RH2 $p=1$, but even a high density of these was not sufficient to stabilize that phase epitaxially or to reduce its energy below that of RH1 $p=1$. Our search for stable, thin ordered regions of SiGe between (001)-oriented layers of Si and Ge, a possibility suggested by Mäder, von Känel, and Baldereschi[46] showed the abrupt (001) Si/Ge interface to be favored over the ordered interdiffused interface.

B. Summary of ordering trends

Before presenting our conclusions regarding the spontaneous ordering of SiGe alloys, we will briefly review the experimental and theoretical work to date. These can be divided into those appropriate to *coherent* (generally thin) SiGe films [strained to match the lattice constant of a substrate, in which case Eq. (15) applies], and those appropriate to *incoherent* (generally thick, with substrate strain relieved by misfit dislocations) SiGe layers [where Eq. (1) applies].

Regarding first *strained* SiGe: Ourmazd and Bean[18] discovered spontaneous ordering into a rhombohedral phase in Si/SiGe SL's grown on (001) Si substrates, though they were unable to determine whether the structure was RH1 $p=1$ or RH2 $p=1$. In their experiment the SiGe film was sufficiently thin to create a coherently strained SiGe structure having the Si lattice parameter parallel to the substrate. They made two important observations: (i) the ordering was not present (or was only very weak) following growth (at 550 °C) but appeared after annealing the samples (at about 450 °C) and cooling them slowly (rapid quenches from that temperature resulted in little ordering), and (ii) they observed that the transition was reversible with temperature cycling. Both observations strongly suggest that the ordering they observed reflects bulk thermodynamics rather than surface thermodynamics or kinetic effects. Lockwood *et al.*[50] confirmed the observation of weak spontaneous ordering in as-grown samples of both Si/SiGe SL's and single epilayers of SiGe grown on (001) Si substrates. They did not observe any significant annealing effects in their experiments. Martins and Zunger[12] (based on first-principles calculations) and Littlewood[15] (based on harmonic VFF calculations) attributed these observations to the RH1 $p=1$ phase, since they found the epitaxial formation enthalpy δH [Eq. (15)] of RH1 $p=1$ on (001) Si to be negative, and since the strain energy of RH2 is much higher than that of RH1. Koiller and Robbins[14] later reached the same conclusion on the basis of a harmonic VFF calculation. Both Littlewood[15] and Koiller and Robbins[14] calculated estimates of the formation enthalpy of the random alloy including only strain energy, and came to the conclusion that the transition temperature so calculated was much too small to account for the $T_c \approx 700$ K observed by Ourmazd and Bean.[18]

Regarding *unstrained* SiGe, LeGoues, Kesan, and Iyer[19] observed ordering in the RH2 $p=1$ phase in thick, *unstrained* SiGe, and speculated that the fact that the chemical energy of RH2 is more favorable than that of RH1 could stabilize it over RH1 even in bulk form. LeGoues *et al.*[51] later presented further studies suggesting that the observation of RH2 ordering in unstrained films was caused by surface thermodynamic processes *during growth,* rather than by bulk thermodynamics. While this is quite possibly the correct explanation of

their observation of RH2 $p=1$ ordering in unstrained SiGe, it cannot account for the reversible, post-growth ordering observed in strained SiGe by Ourmazd and Bean.[18] Indeed Müller *et al.*[52] have recently observed that thin SiGe films grown on either Si or Ge substrates show both RH1 $p=1$ and RH2 $p=1$ ordering in the as-grown sample; on annealing the sample the RH2 order vanishes, while subsequent cooling gives rise to a *reversible* order-disorder transition, with RH1 $p=1$ as the low-temperature ordered phase. This shows the RH1 $p=1$ phase to be the most stable one thermodynamically.

C. Discussion of ordering

From our results, we come to the following conclusions regarding ordering of SiGe. (i) In spite of its more favorable chemical energy, the overwhelmingly higher strain energy of RH2 ensures that RH1 has a lower formation enthalpy both in bulk and when strained coherently on (001) Si. This suggests that the ordered *coherent epitaxial* phase observed by Ourmazd and Bean after annealing was RH1 $p=1$, rather than RH2. Since the reversibility of this ordering has now been substantiated by Müller *et al.*,[52] we can conclude that the post-growth ordering observed in these *strained* phases is not a result of the irreversible surface-induced ordering during growth that has been proposed by LeGoues *et al.*[51] (ii) It also makes clear that the observation of unstrained *bulk* RH2 $p=1$ by LeGoues *et al.*[19] is not due to the low chemical energy of that phase, as they originally suggested. Instead, our results lend support to their more recent proposal[51] of a surface-induced ordering mechanism *during* growth that favors RH2. Such a mechanism would likely also cause initial formation of RH2 in *as-grown* coherent samples as well, as has been confirmed by Müller *et al.*,[52] but subsequent annealing for sufficient time at sufficiently high temperature results[52] in elimination of that high-energy phase. (iii) Our calculations show that the chemical energy favors the random alloy over RH1 $p=1$, in contrast to the opposite trend in the strain energies, making the two structures energetically indistinguishable both in bulk and on (001) Si. If we apply a strain-energy correction for the underestimation of bond lengths and lattice mismatch by the pseudopotential results, the epitaxial [on (001) Si] RH1 $p=1$ structure is slightly more stable than the epitaxial random alloy (which is, in turn, slightly more stable than coherent constituents), but the formation energies are still much too close to account for the order-disorder transition temperature observed by Ourmazd and Bean[18] or Müller *et al.*[52] (iv) The microscopic interactions at the interfaces of a Si/SiGe SL, such as that grown by Ourmazd and Bean,[18] do not substantially alter the predicted order-disorder transition temperature calculated on the basis of a "virtual" substrate calculation of strained SiGe on a (001) Si substrate. (v) Hence, the Ourmazd and Bean[18] experiment remains quantitatively unexplained.

ACKNOWLEDGMENTS

We are grateful to L. G. Ferreira for providing us with a copy of his program for calculating the lattice-averaged pseudospin products and for the initial computation of many of them. Also, we thank R. G. Dandrea for making his results on SiGe available to us, and Dr. K. Mäder and Dr. H. von Känel for providing us copies of their work (Refs. 46 and 52) prior to their publication.

[1]M. Ospelt, W. Bacsa, J. Henz, K. A. Mäder, and H. von Känel, Superlatt. Microstruct. **5**, 71 (1989).

[2]E. Kasper, H. Kibbel, H. Jorke, H. Brugger, E. Friess, and G. Abstreiter, Phys. Rev. B **38**, 3599 (1988).

[3]A. T. Fiory, J. C. Bean, R. Hull, and S. Nakahara, Phys. Rev. B **31**, 4063 (1985); T. P. Pearsall, J. Bevk, J. Bonar, M. P. Mannaerts, and A. Ourmazd, *ibid.* **39**, 3741 (1989).

[4]S. J. Chang, K. L. Wang, R. C. Bowman, and P. M. Adams, Appl. Phys. Lett. **54**, 27 (1989).

[5]E. Friess, H. Brugger, K. Eberl, G. Krötz, and G. Abstreiter, Solid State Commun. **69**, 899 (1989); K. Eberl, G. Krötz, R. Zachai, and G. Abstreiter, J. Phys. (Paris) Colloq. **48**, C5-S11 **48**, C5-329 (1987).

[6]D. Brasen, S. Nakahara, and J. C. Bean, J. Appl. Phys. **58**, 1860 (1985).

[7]T. Narusawa and W. M. Gibson, Phys. Rev. Lett. **47**, 1459 (1981).

[8]S. Froyen, D. M. Wood, and A. Zunger, Phys. Rev. B **36**, 4547 (1987); Appl. Phys. Lett. **54**, 2435 (1989).

[9]S. Froyen, D. M. Wood, and A. Zunger, Phys. Rev. B **37**, 6893 (1988).

[10]T. P. Pearsall, *CRC Critical Reviews on Solid State and Materials Sciences* (Chemical Rubber Company, Boca Raton, FL, 1989), Vol. 15, p. 551; J. Lumin. **44**, 367 (1989).

[11]J. L. Martins and A. Zunger, Phys. Rev. B **30**, 6217 (1984).

[12]J. L. Martins and A. Zunger, Phys. Rev. Lett. **56**, 1400 (1986).

[13]S. Ciraci and I. P. Batra, Phys. Rev. B **38**, 1835 (1988).

[14]B. Koiller and M. O. Robbins, Phys. Rev. B **40**, 12 554 (1989).

[15]P. B. Littlewood, Phys. Rev. B **34**, 1363 (1986).

[16]S.-H. Wei and A. Zunger, Phys. Rev. Lett. **61**, 1505 (1988).

[17]R. G. Dandrea, J. E. Bernard, S.-H Wei, and A. Zunger, Phys. Rev. Lett. **64**, 36 (1990).

[18]A. Ourmazd and J. C. Bean, Phys. Rev. Lett. **55**, 765 (1985).

[19]F. K. LeGoues, V. P. Kesan, and S. S. Iyer, Phys. Rev. Lett. **64**, 40 (1990).

[20]For the rhombohedral structures we use the term "bilayer" to refer to pairs of (111) layers separated by a distance of $a/4\sqrt{3}$ in the diamond structure, where a is the lattice constant. These bilayers are separated from each other by the larger distance $a\sqrt{3}/4$.

[21]There is also a third rhombohedral structure, RH3, which has half-integral p, and one mixed-bilayer and one pure-bilayer interface. This structure has energy intermediate between those of RH1 and RH2 and is not considered here.

[22]J. Ihm, A. Zunger, and M. L. Cohen, J. Phys. C **12**, 4409 (1979).

[23]W. Kohn and L. J. Sham, Phys. Rev. **140**, A1133 (1965).

[24]J. E. Bernard, L. G. Ferreira, S.-H. Wei, and A. Zunger, Phys. Rev. B **38**, 6338 (1988).

[25]For example, Ciraci and Batra (Ref. 13) partitioned the forma-

tion enthalpy into a bulklike strain term analogous to our ΔE_{CS} and an interfacelike term attributed to the chemical process associated with the formation of the Si—Ge bonds at the interface, and hence analogous to our I_{CE}.

[26]P. N. Keating, Phys. Rev. **145**, 637 (1966).

[27]R. M. Martin, Phys. Rev. B **1**, 4005 (1970).

[28]W. H. Press, B. P. Flannery, S. A. Teukolsky, and W. T. Vetterling, *Numerical Recipes* (Cambridge University Press, Cambridge, 1986), pp. 301–306.

[29]A. Zunger, S.-H. Wei, L. G. Ferreira, and J. E. Bernard, Phys. Rev. Lett. **65**, 353 (1990); S.-H. Wei, L. G. Ferreira, J. E. Bernard, and A. Zunger, Phys. Rev. B **42**, 9622 (1990); S. H. Wei and A. Zunger, Appl. Phys. Lett. **56**, 662 (1990); K. Hass, L. C. Davis, and A. Zunger, Phys. Rev. B **42**, 3757 (1990).

[30]S. Froyen, Phys. Rev. B **39**, 3168 (1989).

[31]F. Birch, Phys. Rev. **71**, 809 (1947); J. Geophys. Res. **57**, 227 (1952).

[32]D. M. Wood and A. Zunger, Phys. Rev. B **40**, 4062 (1989).

[33]R. G. Dandrea (private communication).

[34]L. G. Ferreira, S.-H. Wei, and A. Zunger, Phys. Rev. B **40**, 3197 (1989); S.-H. Wei, L. G. Ferreira, and A. Zunger, *ibid.* **40**, 8240 (1990).

[35]J. W. D. Connolly and A. R. Williams, Phys. Rev. B **27**, 5169 (1983).

[36]J. M. Sanchez, F. Ducastelle, and D. Gratias, Physica A **128**, 334 (1984).

[37]In this section we use the term "lattice" in the less strict (but traditional in the literature on cluster expansions) sense of an array of empty sites, with no restriction to being equivalent under the operations of some translation group.

[38]L. G. Ferreira (private communication).

[39]Essentially full convergence for $Si_{0.5}Ge_{0.5}$ is reached with six interactions, including up to fourth-nearest-neighbor pairs and four-body second-nearest-neighbor interactions, though two of these (four-body first-nearest-neighbor and two-body third-nearest-neighbor) are smaller than the others and can be eliminated with little additional error.

[40]S. de Gironcoli, S. Baroni, and P. Giannozzi, in Proceedings of the International Conference on the Physics of Semiconductors, Thessaloniki, 1990, edited by E. M. Anastussakis and J. D. Joannopoulos (World Scientific, Singapore, 1990), Vol. 2, p. 877.

[41]In terms of the excess bond energy δ of the Si—Ge bond relative to equivalent amounts of Si—Si and Ge—Ge bonds, $\Delta E_{\text{chem}}^{(\alpha)} = N_\alpha \delta / N$, where N_α is the number of Si—Ge bonds per unit cell, and N is the number of atoms per unit cell. Since $N_\alpha / N = -\overline{P}_{2,1}$ (Table VI), the excess bond energy is just $\delta = -D_{2,1} J_{2,1}$.

[42]P. C. Kelires and J. Tersoff, Phys. Rev. Lett. **63**, 1164 (1989).

[43]A. Qteish and R. Resta, Phys. Rev. B **37**, 1308 (1988); **37**, 6983 (1988).

[44]G. B. Stringfellow, J. Phys. Chem. Solids **34**, 1749 (1973); G. B. Stringfellow and P. E. Greene, J. Electrochem. Soc. **117**, 1075 (1970).

[45]We have found, for example, that in our calculations with a 20-Ry cutoff energy, the formation enthalpy of the zincblende structure is about 3 meV/atom lower when two special **k** points are used than when ten are used. This is caused by the fact that Ge requires more dense **k**-point sampling to reach convergence than do ZB or Si.

[46]K. A. Mäder, H. von Känel, and A. Baldereschi, Superlatt. Microstruct. (to be published).

[47]Here we use the term "lattice" in the strict sense, meaning a particular set of points, all of which are equivalent under the operations of the translation group of the crystal, rather than the complete set of atomic sites.

[48]The results of Ref. 46 were phrased in terms of the critical value of $-2J_{2,1}$ required to produce epitaxial stability (hence instability of an abrupt Si/Ge interface) of ordered RH1 $p=1$ and RH2 $p=1$ phases, assumed as possible candidates for the phase of the interdiffused interface regions of a (001) Si/Ge SL.

[49]Note that because the thin layers ($q<4$) contain fractional unit cells of the ordered structures, we cannot claim that SQS-8 models a thin disordered region here, though we have shown that it does so for thick layers.

[50]D. J. Lockwood, K. Rajan, E. W. Fenton, J. M. Baribeau, and M.W. Denhoff, Solid State Commun. **61**, 465 (1987).

[51]F. K. LeGoues, V. P. Kesan, S. S. Iyer, J. Tersoff, and R. Tromp, Phys. Rev. Lett. **64**, 2038 (1990).

[52]E. Müller, H.-U. Nissen, K. A. Mäder, M. Ospelt, and H. von Känel (unpublished); see also E. Müller, H.-U. Nissen, M. Ospelt, and H. von Känel, Phys. Rev. Lett. **63**, 1819 (1989).